Harmonic Mitigation and Resonance Damping Based on Impedance Model Using Series LC Filtered VSI

Bai, Haofeng

Publication date:
2017

Document Version
Publisher's PDF, also known as Version of record

HARMONIC MITIGATION AND RESONANCE DAMPING BASED ON IMPEDANCE MODEL USING SERIES LC FILTERED VSI

BY
HAOFENG BAI

DISSERTATION SUBMITTED 2017

AALBORG UNIVERSITY
DENMARK

HARMONIC MITIGATION AND RESONANCE DAMPING BASED ON IMPEDANCE MODEL USING SERIES LC FILTERED VSI

by

Haofeng Bai

AALBORG UNIVERSITY
DENMARK

Dissertation submitted to Faculty of Engineering, Science

Aalborg University

Department of Energy Technology, Aalborg University

Pontoppidanstræde 101, DK-9220 Aalborg East, Denmark

e-mail: hba@et.aau.dk

July 2017

Dissertation submitted:	July, 2017
PhD supervisor:	Prof. Frede Blaabjerg Aalborg University
Assistant PhD supervisor:	Assoc. Prof. Xiongfei Wang Aalborg University
PhD committee:	Tomislav Dragicevic (Chairman) Aalborg University
	Patrick Wheeler University of Nottingham
	Vladimir Katic University of Novi Sad
PhD Series:	Faculty of Engineering and Science, Aalborg University
Department:	Department of Energy Technology

ISSN (online): 2446-1636
ISBN (online): 978-87-7112-987-8

Published by:
Aalborg University Press
Skjernvej 4A, 2nd floor
DK – 9220 Aalborg Ø
Phone: +45 99407140
aauf@forlag.aau.dk
forlag.aau.dk

Printed in Denmark by Rosendahls, 2017

ENGLISH ABSTRACT

The usage of grid-connected Voltage Source Inverters (VSI) enables the Power Electronics (PE) based power system and brings new harmonic issues such as the switching harmonic attenuation for high power VSIs and harmonic instability, where high order harmonic resonance arises from the interactions between the VSIs and the grid impedance. Damping of the resonances becomes important with more VSIs connected to the grid, since they will cause the VSIs to be disconnected undesirably. The series LC filtered VSI, which has been used to emulate virtual impedance at the harmonic frequencies, is effective to dampen the harmonic resonance and stabilize the PE based power system with reduced power rating and dc-link voltage.

Impedance modelling is an effective way to analyze the harmonic interaction within a PE based power system. The Norton equivalent model of a grid-connected VSI consists of a current source, which is determined by the current reference and the closed-loop gain, and the output admittance, which is the transfer function from the disturbance to the output. However, in existing studies on the control of the series LC filtered VSI, the output admittance is often neglected, which leads to some limitations in the applications. For the series LC filtered active damper, the resonance frequency should be calculated online in order to tune the current controller; for the series LC filtered Resistive-Active Power Filter (R-APF), the harmonic voltages must be measured to obtain the current reference. Active Power Filtering (APF) for the switching harmonic attenuation of the high power VSI with low switching frequency is also challenging due to the limited current control bandwidth of the VSI.

In this thesis, the operation principles of the series LC filtered VSI are investigated for three objectives: 1) harmonic stabilization of PE based power system, 2) switching harmonic attenuation of the high power VSI with low switching frequency and 3) resistance emulation at low order harmonics. All the control strategies derived in this thesis are based on the impedance model of the series LC filtered VSI. In order to stabilize the PE based power system, impedance based stability analysis of the PE based power system is first carried out, which indicates that the negative real part of the output admittance of the VSIs are the origin of the instability. Instead of mimicking the behavior of a resistor, the operating principle of the active damper is changed to enhance the passivity of the system. A simple control scheme based on a proportional current controller and a low-pass filter is also proposed for the active damper. Since the resonant current controller is not needed, the online detection of the resonance becomes unnecessary.

The physical representation of the current controller of the series LC filtered VSI is further studied with the help of Thevenin equivalent circuit. In the output impedance, virtual resistance and capacitance can be introduced by proportional and integral current controllers, respectively. An output impedance shaping method that

introduces zero output impedance is also proposed. With the proposed output impedance shaping method, the series LC filtered VSI can be used to bypass the switching harmonics of the high power VSI, whose frequency range is at kilo Hertz level. Compared with the traditional high frequency APF, the current reference of the Active Trap Filter (ATF) is set to zero and the design of the current controller is much easier. A low order harmonic compensation method for the high power VSI is also proposed. With the proposed ATF, the output current of the high power VSI maintains sinusoidal even in the presence of a distorted grid voltage.

In order to dampen the low order harmonic resonance, an AC voltage sensorless R-APF is proposed. Instead of tracking a special current reference obtained from the harmonic voltage information, the output impedance of the series LC filtered VSI is used to emulate the damping resistance. Thus, the harmonic voltage does not need to be measured. Also, a fundamental voltage estimation method is proposed, which allows the DC-link voltage control. As a result, the AC voltage sensor can be removed in the R-APF. The system cost of the R-APF can be reduced and the isolation between the control circuit and the power circuit can be improved.

It is concluded at the end of this thesis that the impedance model of the series LC filtered VSI offers more possibility to mitigate the harmonics in a power electronics based power system.

Keywords: Power electronics, harmonics, grid-connected voltage source inverter, series LC filter, impedance model, high power, active power filter, stability, resonance, passivity, switching harmonic attenuation, resonance damping.

.

DANSK RESUME

Brug af net-tilsluttede spændings-kilde baserede invertere (VSI) gør det muligt at udvikle effekt elektronisk (PE) baserede el-systemer, men det giver også nye harmoniske problemer såsom at dæmpe harmoniske af switchningerne samt harmonisk ustabilitet, hvor højere ordens harmoniske resonanser udspringer af interaktioner mellem VSIer samt impedansen i el-nettet. Dæmpning af resonanser bliver vigtigt med flere VSIs tilsluttet til el-nettet, da de uønsket vil forårsage VSIs til at blive afbrudt. En serieforbundet LC filtreret VSI, som er blevet brugt til at emulere virtual impedans ved de harmoniske frekvenser, er effektiv til at dæmpe de harmoniske resonanser og stabilisere det PE baserede el-system med reduceret effekt rating og dc-link spænding.

Impedans modellering er en effektiv måde at analysere den harmoniske interaktion i et PE baseret el-system. En ækvivalent Norton model af en net-tilsluttete VSI består af en strømkilde, som bestemmes af strøm referencen, det lukkede kredsløbs forstærkning, og output admittans, som er overførselsfunktionen fra forstyrrelsen til outputtet. Men i eksisterende undersøgelser af kontrol af serie-forbundne LC filtreret VSI, output admittansen er ofte negligeret, hvilket fører til nogle begrænsninger i anvendelsen. For en serieforbundet LC filtreret aktiv dæmper, on-line målinger af resonansfrekvenser er nødvendig for at kunne designe strøm kontrolleren og for serie-forbunden LC filtreret resistente-aktiv Power Filter (R-APF), de harmoniske spændinger skal måles for at opnå en strøm reference. En Aktiv Power Filtrering (APF) af den skiftende harmoniske dæmpning af høj effekt VSI med lav switch frequency er heller ikke let på grund af den begrænsede strømkontrol båndbredde af VSIer.

I denne afhandling, er principperne for serie-forbundne LC filtreret VSI undersøgt for tre for mål: 1) harmonisk stabilisering af PE baseret el-system, 2) skiftende harmonisk dæmpning af højeffekt VSI med lav switch frequency og 3) modstands emulering ved lav ordens harmoniske. Alle de kontrolstrategier, der er udledt i dette afhandling, er baseret på impedans modellen for serie-forbundne LC filtreret VSI. For at stabilisere et PE baseret el-system, er en impedans baseret stabilitetsanalyse af et PE baseret el-system først foretaget, som angiver at den negative reelle del af output admittansen af VSIer og som er grunden til ustabiliteten. I stedet for at efterligne opførslen af en modstand, er arbejdsprincippet for den aktive dæmper ændret for at forbedre passiviteten af systemet. En simpel kontrolstrategi baseret på proportional strøm-kontrollere og et lav-pass filter er også foreslået for den aktive dæmper.

Den fysiske repræsentation af strøm-kontrolleren for den serie-forbundne LC filtreret VSI er yderligere undersøgt ved hjælp af et ækvivalent Thevenin kredsløb. I output impedansen kan virtuelle modstande og kondensator indføres af hhv. proportional og integrerende strøm-kontrollere. Der foreslås også en udgangs

impedance formende metode, der introducerer ingen output impedans. Med den foreslåede udgangs impedans formende metode, kan den serie-forbundne LC filtreret VSI bruges til at omgå de skiftende harmoniske af høj-effekt VSI, hvis frekvensområde er i kilo Hertz området. Sammenlignet med den traditionelle højfrekvente APF, er strøm referencen til den Aktive Trap Filter (ATF) angivet til nul, og design af strøm-kontrolleren er meget lettere. En lav ordens harmonisk kompensations metode for høj-effekt VSIer foreslået med ATF baseret på impedans modellen af systemet. Med det foreslåede princip fastholdes output strømmen af høj-effekt delen af VSI selv i det tilfælde miden forvrænget spænding i elnettet.

For at dæmpe lav ordens harmoniske resonanser er en resistente-aktiv Power Filter uden spændingssensorer også foreslået. I stedet for at bruge en særlig strømreference beregnet ud fra oplysninger om harmoniske spændinger, er output impedansen af det serie-forbundne LC filtreret VSI brugt til at emulere en dæmpningsmodstand. Den harmoniske spænding skal således ikke måles. Derudover foreslås en spænding estimering metode, som muliggør en DC-link spændings kontrol i konverteren. Som et resultat, kan AC spændings-sensoren fjernes i R-APF. System omkostninger af R-APF kan derved reduceres og isoleringen i mellem styringskredsløbet og effekt kredsløb et kan derved forbedres.

Det konkluderes i slutningen af denne afhandling, at impedans modellen af en serieforbundet LC filtreret VSI tilbyder flere muligheder for at dæmpe harmoniske i et effektelektronik baseret el-system og vil være et potentiale konverter i fremtidens el-system.

Nøgleords: Power elektronik, harmonier, net-tilsluttede spænding kilde inverter, serieforbundet LC filter, impedans model, høj effekt, aktive power filter, stabilitet, resonans, passivitet, skiftende harmonisk dæmpning, resonans dæmpning.

Thesis Title: Harmonic Mitigation and Resonance Damping Based on Impedance Model Using Series LC Filtered VSI

Ph. D. Student: Haofeng Bai

Supervisor: Prof. Frede Blaabjerg, Aalborg University

Co-supervisor: Assoc. Prof. Xiongfei Wang, Aalborg University

Publications in Refereed Journals

- **H. Bai**, X. Wang, P. C. Loh and F. Blaabjerg, "Passivity enhancement of grid-tied converters by series LC-filtered active damper," *IEEE Trans. Ind. Electron.*, vol. 64, no. 1, pp. 369-379, Jan. 2017.
- **H. Bai**, X. Wang, P. C. Loh and F. Blaabjerg, "An active trap filter for switching harmonics attenuation of low-pulse-ratio inverters," *IEEE Trans. Power. Electron.*, early access.
- **H. Bai**, X. Wang, and F. Blaabjerg, "Passivity enhancement in RES based power plant with paralleled grid-connected inverter," *IEEE Trans. Ind. Appl.*, vol. 53, no. 4, 3793-3802, July-Aug. 2017.
- **H. Bai**, X. Wang, and F. Blaabjerg, "A Grid-voltage-sensorless resistive active power filter with series LC-filter," *IEEE Trans. Power. Electron.*, early access.
- **H. Bai**, X. Wang, P. C. Loh and F. Blaabjerg, "Harmonic analysis and mitigation of low-frequency switching VSIs with an active trap filter," *IEEE J. Emerg. Sel. Top. Power Electron.*, submitted.

Co-authored Journal Publications:

- C. Yoon, **H. Bai**, R. N. Beres, X. Wang, C. L. Bak and F. Blaabjerg, "Harmonic stability assessment for multi-paralleled, grid-connected inverters," *IEEE Trans. Sustainable Energy*, vol. 7, no. 4, pp. 1388-1397, Oct. 2016.
- Y. Geng, Y. Yun, R. Chen, K. Wang, **H. Bai**, and X. Wu, "Parameters design and optimization for LC-type off-grid inverter with inductor-current-feedback active damping," in *IEEE Trans. on Power Electron.*, vol. PP, no.99, pp.1-1
- L. Harnefors, R. Finger, X. Wang, **H. Bai**, and F. Blaabjerg, "VSC input-admittance modeling and analysis above the Nyquist frequency for passivity-based stability assessment," in *IEEE Trans. on Power Electron.*, vol. PP, no.99, pp.1-1

Publications in Refereed Conferences

- **H. Bai**, X. Wang, P. C. Loh and F. Blaabjerg, "Passivity enhancement of grid-tied converter by series LC-filtered active damper," *2015 IEEE Energy Conversion Congress and Exposition (ECCE)*, Montreal, QC, 2015, pp. 5830-5837.
- **H. Bai**, X. Wang, P. C. Loh and F. Blaabjerg, "An active trap filter for high-power voltage source converters," *2015 IEEE 6th International Symposium on Power Electronics for Distributed Generation Systems (PEDG)*, Aachen, 2015, pp. 1-8.
- **H. Bai**, X. Wang and F. Blaabjerg, "Passivity enhancement by series LC filtered active damper with zero current reference," *2016 IEEE 8th International Power Electronics and Motion Control Conference (IPEMC-ECCE Asia)*, Hefei, 2016, pp. 2937-2944**.**
- **H. Bai**, X. Wang, and F. Blaabjerg, "Passivity enhancement in RES based power plant with paralleled grid-connected inverter," *2016 IEEE Energy Conversion Congress and Exposition (ECCE)*, Milwaukee, WI, 2016, pp. 1-8.
- **H. Bai**, X. Wang, P. C. Loh and F. Blaabjerg, "A series-LC-filtered active trap filter for high power voltage source inverter," *2016 IEEE Energy Conversion Congress and Exposition (ECCE)*, Milwaukee, WI, 2016, pp. 1-8.
- **H. Bai**, X. Wang, P. C. Loh and F. Blaabjerg, "Harmonic analysis and mitigation of low-frequency switching voltage source inverter with series LC filtered VSI," *2017 IEEE Applied Power Electronics Conference and Exposition (APEC)*, Tampa, FL, 2017, pp. 3299-3306. .

ACKNOWLEDGEMENT

This thesis summarizes the Ph. D project "Harmonic Mitigation and Resonance Damping Based on Impedance Model Using Series LC Filtered VSI", which is carried out during the last three years. The Ph. D project is supported mainly by China Scholarship Council (CSC) and partially by the Department of Energy Technology, Aalborg University, Denmark and the European Research Council (ERC). Acknowledgement are given to the above-mentioned institutions.

First of all, I would like to express my sincere gratitude to my supervisors, Professor Frede Blaabjerg and Associate Professor Xiongfei Wang. Their rich engineering experience, great patience and encouragement made my research productive and motivating. Furthermore, I want to thank Professor Poh Chiang Loh from the Chinese University of Hong Kong. During his stay in Aalborg University, we had many fruitful discussions which stimulated a lot of ideas.

Then, I want to thank my team mates in the Harmony project, Professor Claus Leth Bak, Dr. Remus Narcis Beres, Dr. Changwoo Yoon, Dr. Junbum Kwon, Dr. Zhen Xin, Dr. Minghui Lu, Mr. Dapeng Lu and Mr. Esmaeil Ebrahimzadeh, and Mr. Mohammad Kazem Bakhshizadeh. They gave me valuable feedbacks on my project report in the monthly team meetings. I also want to thank all my friends in Aalborg, who make the life after work interesting with all the footsball and basketball games. I wish all the best for their future career and life.

Also, I want to express my thanks to all the academic and administrative stuff in the Department of Energy Technology for their marvelous help on the scientific as well as organizational issues. Thank Mr. Andreas Larsen, who helped me a lot with my Danish translation and will start his master study in AAU soon. Work and life become much easier for me with their help.

Finally, the most important and the sincerest gratitude to my wife and my parents for their exceptional love and their encouragement through my life. Research is an adventure into an unknown world and sometimes requires sacrifices and support from the families.

Haofeng Bai
July, 2017
Aalborg East, Denmark

TABLE OF CONTENTS

CHAPTER 1. INTRODUCTION

1.1. HARMONIC ISSUES IN POWER ELECTRONICS BASED POWER SYSTEM

Nowadays, the Power Electronics (PE) based power converters are widely used in the power systems, enabling the "PE based power systems" as mentioned in many literatures [1]-[5]. A typical structure of the PE based power system is shown in Fig. 1-1. Compared with traditional AC power systems, various PE based converters, especially the Voltage Source Inverters (VSI), as well as many linear and non-linear loads are connected to the main grid. On the generation side, the PE based power system allows more types of energy sources to be connected to the grid, such as the wind and the solar energy [16]-[21]. On the load side, the PE based power converters improve the controllability and input power factor of the load, such as the AC motor drive and Power Factor Correction (PFC) rectifiers [24]-[32]. The harmonics are the sine-shaped oscillations in the voltage and current whose frequency is an integral multiple of the fundamental frequency. Like the traditional power system, the PE based power system is challenged by harmonics. The effects of the harmonic voltage and current can be summarized as follows [6]-[8], [11]-[13]. Standards have been established regarding the amplitude of the harmonics, some of which are listed in Table 1.1 and Table 1. 2, and they are continuously emerging.

- Mechanical vibration of the motor;
- Increased loss and overheating of transformers;
- Series and parallel harmonic resonance in the system voltage;
- Undesired trigger of the power system protection.

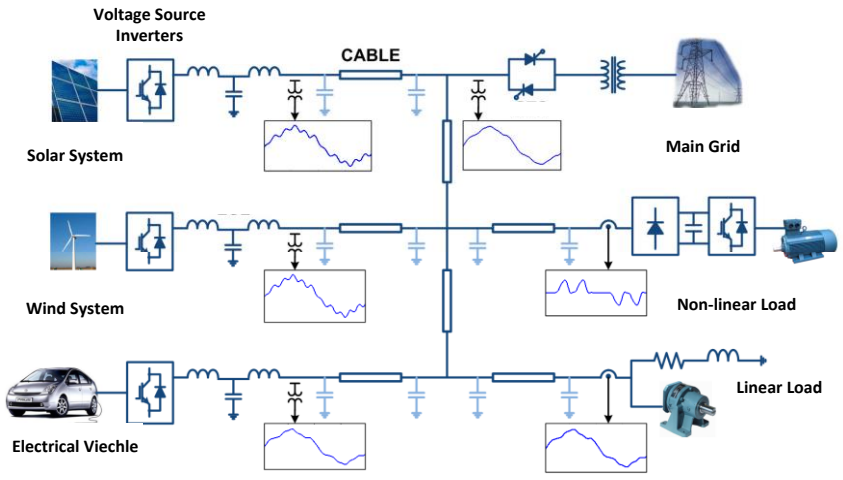

Figure 1-1. Power Electronics based power system with connection to the main grid.

Table 1.1 Harmonic current limits (% of rated current)

Harmonic order *h*	IEEE 519[1] [LV & MV]	IEC 61000-3-2[2] [LV]	IEC 61000-3-12 [LV]	BDEW[3] [MV]	GB 14549 [LV & MV]
3	4	14.4	-	-	8.16
5	4	8.8	10.7	2.06	14.1
7	4	4.8	7.2	2.84	10
11	2	2	3.1	1.8	6.38
13	2	7.5/*h*	2	1.32	5.47
17	1.5	7.5/*h*	-	0.76	0.76
19	1.5	7.5/*h*	-	0.62	0.62
23	0.6	7.5/*h*	-	0.42	0.42
25	0.6	7.5/*h*	-	0.32	0.32
29-33	0.6	7.5/*h*	-	8.67/*h*	8.67/*h*
35-37	0.3	7.5/*h*	-	8.67/*h*	8.67/*h*
41-49	0.3	-	-	6.24/*h*	6.24/*h*
53-179	-	-	-	6.24/*h*	6.24/*h*

[1] $I_{SC}/I_L < 20$, where
I_{SC} = maximum short-circuit , and
I_L = maximum demand load current under normal operating condition.
[2] Base current is set to 16A.
[3] Calculated for 400 V and I_{SC}/I_L =20

Table 1.2 Harmonic voltage limits (% of rated voltage)

Harmonic order *h*	EN 61000-2-2[1] [LV]	EN 50160 [LV & MV]	BDEW[2] [MV]	GB 14549[3][4] [LV & MV]
3	5	5	-	4
5	6	6	0.5	4
7	5	5	1	4
11	3.5	3.3	1	4
13	3	2	0.85	4
17	2	1.5	0.65	4
19	1.8	1.5	0.6	4
23	1.4	1.5	0.5	4
25	1.3	-	0.4	4
29-37	38.6/*h*-0.27	-	0.4	4

[1] only odd harmonics are considered above 29th.
[2] only odd harmonics are considered between 29th ~ 37th.
[3] specified for 0.38 kV system.
[4] only odd harmonics are considered between 29th ~ 37th.

Based on whether the harmonics are introduced by the harmonics sources or by the stability issues in the PE based system, the harmonics can be categorized into the following two classes.

- Source-related harmonics
- Stability-related harmonics.

1.1.1. SOURCE-RELATED HARMONICS

The source-related harmonics can be introduced by both the non-linear behavior of Line Commutated Converters (LCC) and the fast switching behavior of the PE based power converters.

1) LCC originated harmonics. Most harmonic pollution in the power system comes from LCC-fed loads, such as the diode rectifiers [39] and the thyristor converters. Low-order harmonic currents are generated by these loads, which in turn distort the feeder voltage. Among the LCC-fed loads, the diode rectifiers are the most widely used one. The characteristic harmonic orders of the diode rectifier are [2], [4]-[6], [9]

$$h = kq \pm 1, \quad k = 1, 2, 3... \tag{1.1}$$

where q is the number of pulses. It should be noted that the dominating harmonics generated by an LCC are usually below 40^{th} order [6]-[8].

2) Switching harmonics. The switching frequencies of VSIs range from several hundred Hertz to hundreds of kilo Hertz [40], [41]. Electromagnetic Interference (EMI) can be introduced by the switching ripple of the output current of the VSIs. For the widely used Pulse Width Modulated (PWM) Voltage Source Inverters (VSIs) and the PFC rectifier, the spectrum of the switching harmonics are distributed at the sidebands of the integer times of the switching frequency [40]. Passive filters are widely used to attenuate the switching harmonics is most cases.

1.1.2. STABILITY-RELATED HARMONICS

Compared with the LCCs, the PWM VSIs provide people more flexibility to control the terminal voltage and the output current of the converters. Unfortunately, the closed-loop controlled systems inevitably introduce stability issues [22]-[25], [33]-[39]. For the PE based power converters, the unstable operation of different control loops can introduce harmonic resonances at different frequency ranges [51]-[59]. Based on the frequency range, the stability-related harmonics can be roughly categorized into two classes, namely the harmonic resonance and the near-synchronous resonance [22], [57], [59].

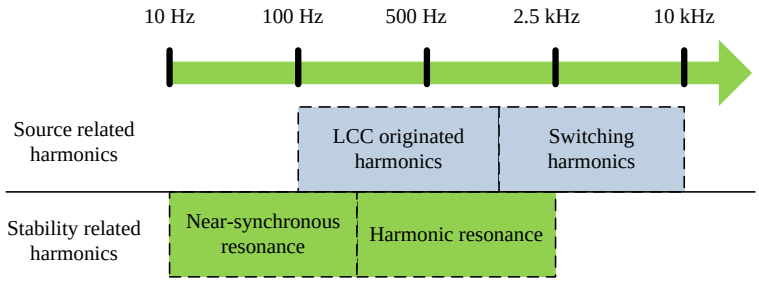

Figure 1-2. Frequency ranges of different harmonics in the PE based power system.

1) Harmonic resonance. The harmonic resonance ranges from several hundred Hertz to several kilo Hertz [22]. This kind of resonance is introduced by the instability of the inner control loops, i.e. current control loop for the VSIs or the AC voltage control loop for the Current Source Inverters (CSIs) [14], [22], [23], [33]-[38]. The main causes for these harmonic instabilities are the total time delay in the control loop and the grid impedance.

2) Near-synchronous resonance. The near-synchronous resonance ranges from below fundamental frequency to roughly several hundred hertz [22]-[25]. This kind of harmonic resonance is mainly introduced by the outer control loops of the converters, such as the PLL and the dc-link control loop [18], [22]-[25], [54].

The frequency ranges of the harmonics in a PE based power system are roughly illustrated in Figure 1-2.

1.2. BACKGROUND TO HARMONIC FILTERING & RESONANCE DAMPING

For the LCC-originated harmonics, both the Passive Power Filter (PPFs) and the Active Power Filters (APF) technologies have been well established. For the stability-related harmonics, a lot of research have been carried out for stabiltiy analysis and improvement of the grid-connected VSIs.

1.2.1. LCC-ORIGINATED HARMONICS MITIGATION

1) Passive Power Filters. The PPFs have long been used due to their low cost and high efficiency [60], [61], [65]-[67]. For most LCC-fed loads, the harmonics are mainly located at the characteristic orders in the frequency domain [4]-[6]. The PPFs use LC branches to form series or parallel resonances at the characteristic frquencies. Basic structures of the PPFs include the tuned trap filters and high pass filters [65].

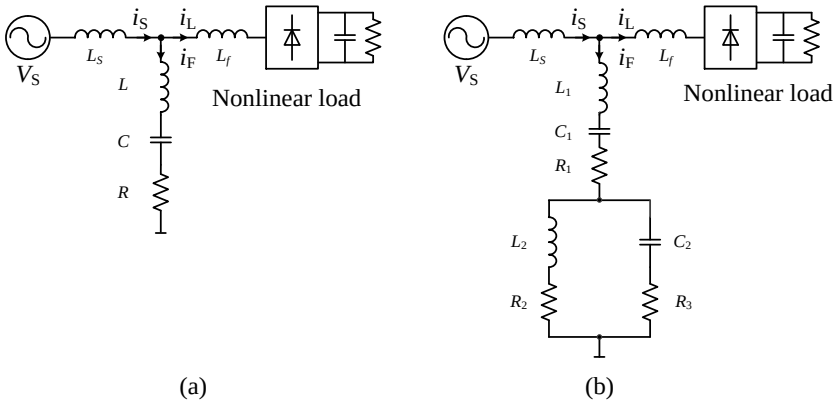

Figure 1-3. Passive tuned filters: (a) single tuned filter, and (b) double tuned filter.

The structures of single and double tuned PPFs are shown in Figure 1-3. Though the PPFs are robust and cost-effective, they have their shortcomings, which can be summarized as [61], [65]–[67]:

- The performance of the PPFs is dependent on the network impedance [65];
- The capacitors in the filters introduce harmonic resonance with the load and network impedance [67];
- The tolerance and the degradation effect of the passive components can also lead to detuning of the filters [61].

2) Active Power Filters. The APFs use a PE based power converter to generate the desired output current or voltage. The APFs can be integrated into the system in series or in parallel, or in both forms [69], which is denoted as the Unified Power Quality Conditioner (UPQC) [70]. Compared with the Current Source Inverters (CSIs), most APF applications adopt the VSI since it has a higher efficiency. The structures of the series APF, shunt APF and the UPQC are shown in Figure 1-4.

The shunt APFs can be installed in the power system without shutting down the power line and compensate the harmonic current directly. For the harmonic voltage source, the shunt APF will increase the magnitude of the load harmonic current [68]. The series APF is connected to the power line through the matching transformer. The series APF is not fit for harmonic current sources, however, it can be used together with the PPFs [63], [68]–[70]. The UPQC is fit for both harmonic voltage source and harmonic current source. The main drawbacks of the UPQC are its high hardware cost [69] and complicated structure.

The basic operation principles of the shunt APF are shown in Figure 1-5. The shunt APF can be controlled either in the current compensating mode or the Resistive-APF

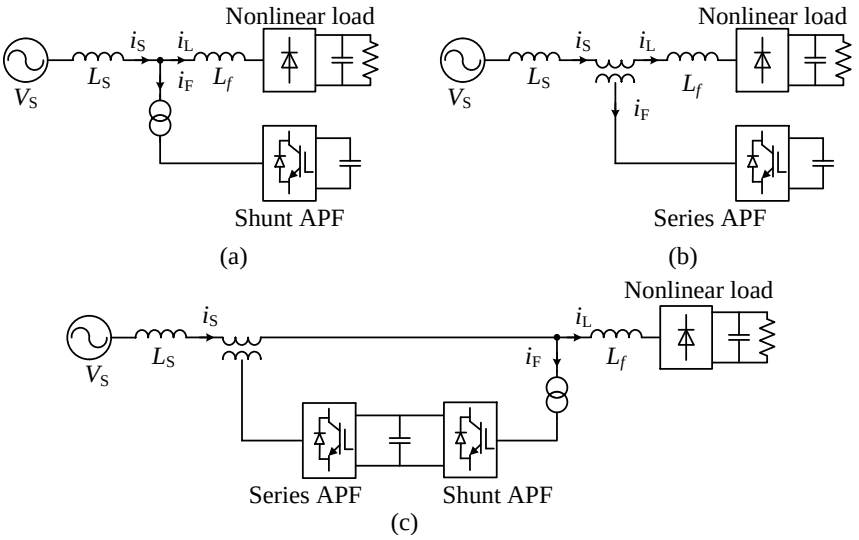

Figure 1-4. Active Power Filters (APF), (a) shunt APF, (b) series APF, and (c) Unified Power Quality Conditioner (UPQC).

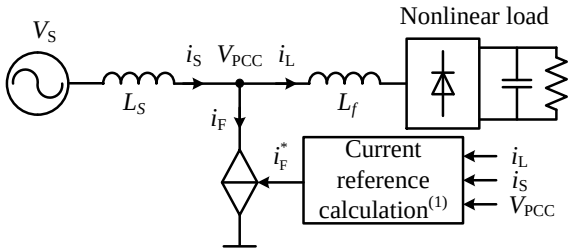

(1) For current compensating APFs i_F^* is calculated with (1.2)
For Resistive-APFs i_F^* is calculated with (1.3)

Figure 1-5. Operation principles of the shunt APF.

(R-APF) mode [74]–[76]. In the current compensating mode, the APF controls its output currents so that they are in the opposite phase with the load harmonic currents. Either the i_S (feedback control) or i_L (feedforward control) is measured to formulate the current reference i_F^* [77]. The harmonic current can be extracted with a low-pass filter or a band-pass filters [78].

$$i_F^* = \begin{cases} K_c i_{Sh} & \text{feedback control} \\ -i_{Lh} & \text{feedforward control} \end{cases} \tag{1.2}$$

For the R-APFs, the output current of the APF is controlled in order to mimic the behavior of a virtual resistor at the harmonic frequencies. The R-APF is effective at isolating the harmonic voltage from propagating through the transmission line [75], [76], [79]–[81]. The current references of the R-APFs are obtained by dividing the harmonic voltage with a virtual resistor, as given by (1.3). The R-APF allows the distributed damping of the resonance without communication between the R-APFs [81]–[83], and has been widely adopted to limit the THD of the feeder voltage and dampen the low order harmonic resonances.

$$i_{\mathrm{F}}^{*} = \frac{1}{R_{\mathrm{d}}} V_{\mathrm{PCCh}} \tag{1.3}$$

3) Hybrid Active Power Filters (HAPFs). The Hybrid-APFs (HAPF) are the combination of APFs and the tuned PPFs [80], [84]–[87]. Compared with the APFs, the HAPFs have lower power rating of the VSI and hence lower cost. Even though many topologies have been proposed for the HAPFs, a capacitor that sustains the bulk of the PCC voltage can be found in many of them. The terminal voltage of the VSI is greatly reduced by the capacitor, which leads to a reduced dc-link voltage and the voltage stress of the semiconductor switches. There are mainly two topologies of the HAPFs, which are named the type I HAPF and the type II HAPF in some literatures [88], [89]. The topologies of type I HAPF and type II HAPF are shown in Figure 1-6 (a) and Figure 1-6 (b), respectively.

For the type I HAPF, the VSI is connected to the PCC through a series LC filter. The advantage of the type I HAPF is that the filter current i_{F} is directly controlled by the HAPF. However, all the fundamental current flows through the VSI and startup resistors are needed to limit the inrush current. The power rating of the type I HAPF is typically 70% lower than the traditional APFs shown in Figure 1-2 (a) [89]. For type II HAPF, the VSI is connected in parallel with the filter inductor. The reactive current is shared between the VSI and the filter inductor. Compared with type I HAPF, the current rating of the VSI for type II HAPF can be even lower [89]. However, the filter current i_{F} cannot be directly controlled by the shunt APF.

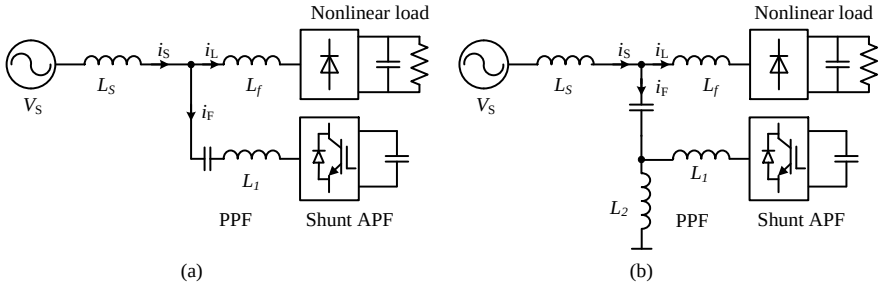

Figure 1-6. Topologies of the Hybrid APF, (a) HAPF type I, and (b) HAPF type II.

1.2.2. SWITCHING HARMONIC MITIGATION

1) Passive filters. The simplest passive filter for the switching harmonic attenuation is an *L* filter, which is shown in Figure 1-7(a). The frequency response of the *L* filter is given by (1.4) and shown in Figure 1-7(b), where a -20 dB/decade attenuation ratio can be observed. Larger inductor is needed for better harmonic filtering. Although it is simple and robust, the L filter is bulky and costly compared with the high order filters [45].

$$Y_L = \frac{1}{L_1 s} \tag{1.4}$$

The LCL filter provides much better performance than the L filter with the same size of passive components [43]-[45]. The structure of an LCL filter is shown in Figure 1-8(a). The shunt capacitor provides a low impedance path for the switching harmonics. The frequency response of the LCL filter is given by (1.5) and shown in Figure 1-8(b), where a -60 dB/decade of attenuation ratio can be observed above the resonance of the LCL filter, or the cross-over frequency. At the resonance frequency, there is a peak, which may destabilize the control system of the converter [44]-[46]. In order to achieve satisfying attenuation of the switching ripples, the resonance frequency should be tuned between 1/6 and ½ of the switching frequency [44].

$$\begin{aligned} Y_{LCL} &= \frac{1}{sC\left(s^2 + \omega_r^2\right)}, \\ \omega_r &= \sqrt{\frac{L_1 + L_2}{CL_1L_2}}. \end{aligned} \tag{1.5}$$

For high power applications, it is sometimes difficult for the LCL filter to tune its resonance frequency well below the switching frequency yet above the desired current control bandwidth [51]. For VSIs with constant swithcing frequency, the LLCL filter can be used. The structure of an LLCL filter is shown in Figure 1-9(a). At the resonance of the LC branch, the impedance is close to zero and the switching ripple can be bypassed by the LC branch. The frequency characteristic of the LLCL filter is given by (1.6) and shown in Figure 1-9(b). There is also a resonance peak, which may lead to instability of the current control loop. Above the resonance frequency, the harmonic attenuation rate is -20 dB/decade.

$$\begin{aligned} Y_{LLCL} &= \frac{L_3Cs^2 + 1}{C\left[L_1L_2 + \left(L_1 + L_2\right)L_3\right]s\left(s^2 + \omega_r^2\right)}, \\ \omega_r &= \sqrt{\frac{L_1 + L_2}{C\left[L_1L_2 + \left(L_1 + L_2\right)L_3\right]}}. \end{aligned} \tag{1.6}$$

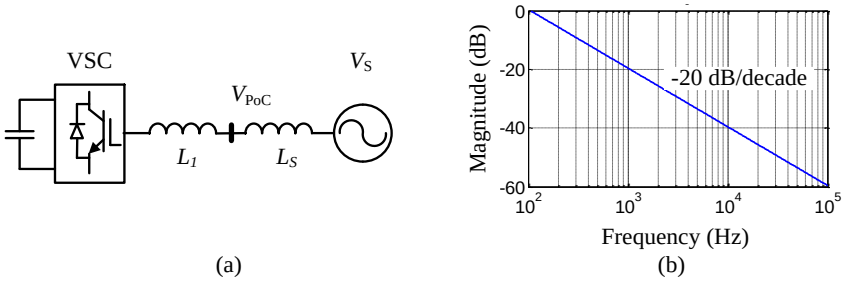

Figure 1-7. L filter, (a) structure of an L filtered VSI, and (b) Bode plot of admittance of the L filter.

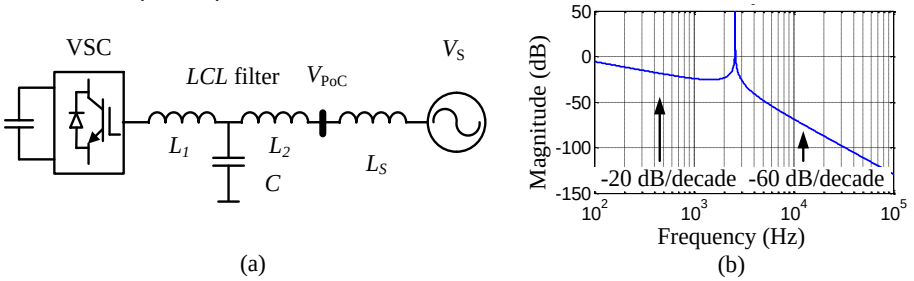

Figure 1-8. LCL filter, (a) structure of an LCL filtered VSI, and (b) Bode plot of admittance of the LCL filter.

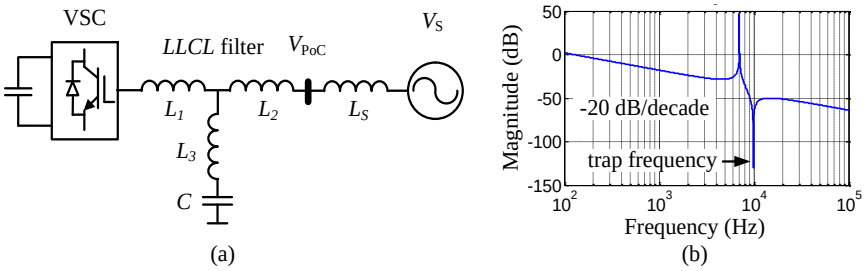

Figure 1-9. LLCL filter, (a) structure of an LLCL filtered VSI, and (b) bode plot of admittance of the LLCL filter.

2) Active filters. For the high power VSIs with low pulse-ratio, the application of the passive filters is challenged by the following issues:

- The sideband harmonics of the switching harmonics are not concentrated in the frequency domain [40] , especially where the system frequency is high, e.g., motor drive system and power system on an airplane;

- The Variable Switching Frequency (VSF) VSIs are becoming popular due to the excellence in reducing the switching loss, EMI noise and acoustic noise [90]–[92]. The passive trap filters cannot be adopted for the VSF VSIs due to their fixed frequency characteristic.

In order to solve the problems of the passive filters, active filters have been proposed for the high power VSIs [62]–[64]. The direct manner is to use a shunt VSI based APF to compensate the switching harmonics generated by the high power VSI. The topology of such a system is shown in Figure 1-10 [63]. The operation principle of the APF in Figure 1-10 is given by

$$i_{\mathrm{F}} = -i_{\mathrm{SW}} . \tag{1.7}$$

It should be noted that the frequencies of the switching harmonics can go up to several kilo Hertz, which is much higher than the low order harmonics seen by the power system. Considering the fact that the common operation frequency of the IGBT is below 20 kHz, accurate closed-loop current control at this frequency range

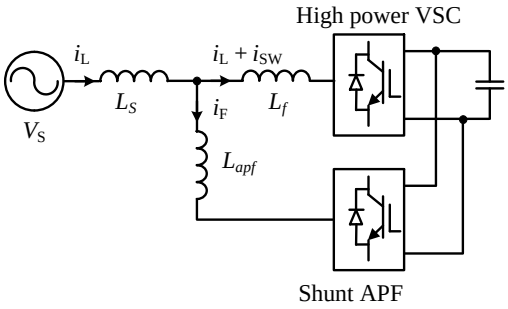

Figure 1-10. System topology of high power VSI with VSI based shunt APF.

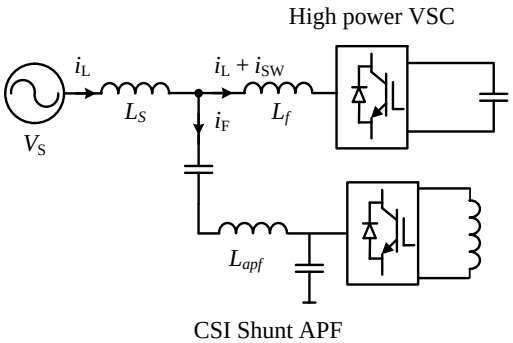

Figure 1-11. System topology of high power VSI with CSI based shunt APF.

is not trivial. Also, the accurate switching harmonic measurement is challenging due to the low Signal-Noise-Rate (SNR) at the switching harmonic frequencies. In order to achieve a high current control bandwidth, the Current Source Inverter (CSI) is used as the power converter for the shunt APF in [63], [64]. The topology of the system with CSI based shunt APF is shown in Figure 1-11. Even though the current regulation is fast for the CSI, the dc-link inductor increases the system cost and weight, which are the inherent disadvantages of the CSI.

1.2.3. STABILITY ENHANCEMENT OF PE BASED POWER SYSTEMS

Due to the better harmonic attenuation capability, the LCL filter and other high order filters are widely used [14]. The capacitive components of the filters are able to introduce harmonic resonance, or the harmonic instabilities, if the grid impedance is high [38].

The problem of harmonic instability has not raised much attention until recent years, when several accidents cause the grid-connected VSIs to be disconnected undesirably from the grid. In Dutch distribution network with high penetration of PV generation, inverters were switched off due to the interactions between the inverters and the grid impedance [35]. In Switzerland, a large number of locomotives were shut down, when an unusually high concentration of active-front-end (i.e., VSI-equipped) locomotives, triggered the resonance destabilization [34].

Researches have been focused on the stability analysis of the grid-connected VSIs and the stability enhancement of the grid-connected VSIs, which includes the passive damper design, active damping control of grid-connected VSIs and the active damper for PE based power system.

1) Stability Analysis of Grid-Connected VSIs. Many modeling methods are proposed to analyze the stability of grid-connected VSIs. Among them, the Root-Locus Analysis (RLA) [95] and the Impedance Based Stability (IBS) methods [38] are the dominating ones. With the RLA method, the grid impedance is integrated into the plant model of the VSI, and the root-locus is investigated to see if there are roots in the right hand side in the *s*-domain or outside the unit cycle in the *z*-domain. The advantages of the RLA method are that the system damping ratio and system resonance frequency can be observed directly. For multiple VSI system, the transfer matrix can be deduced and the eigenvalues of the matrix are calculated. The system resonance modes and damping ratio of each mode can be obtained like described in [96]–[98]. The disadvantages of the RLA method are that the exact grid impedance value needs to be obtained, which is not practical for large and complicated systems. Also, the order of the transfer matrix increases with the number of energy-storing components in the system. As a result, the modelling of the system becomes very complex for paralleled VSIs with different parameters and sampling rates.

For the IBS method, the output admittance (impedance) of the VSIs is deduced considering both the output filter and the current controller of the VSI. The impedance ratio between the VSI and the network is investigated using the Nyquist plot. The Nyquist Criterion can be applied to the impedance ratio [38]. The advantage of the IBS method is that the large scale system can be split into small subsystems[14], [36], [38], [99]–[101]. The modelling of each subsystem is simple and can be used to form the impedance model of the full system. Also, the detailed grid impedance value in not needed to identify the stability. The disadvantage of the IBS method is that it is difficult to use the IBS method to calculate the damping ratio and resonance mode.

2) Passive Damper of Grid-Connected VSIs. Passive damping is the most widely used method to improve the stability of LCL filtered VSIs. The target of the passive damping is to reduce the peak value of the admittance shown in Figure 1-8(b). The simplest damping manner is to insert a resistor in series with the filter capacitor, which is shown in Figure 1-12(a). All the reactive current flows through the resistor, leading to a great amount of power loss [42], [102]. Also the harmonic filtering performance is deteriorated, since the impedance of the capacitor branch is increased. Other passive damping methods are proposed to reduce the power loss and improve the filtering performance, which are shown in Figure 1-12(b)~(f). Nevertheless, the method increases the system cost and reduce the efficiency.

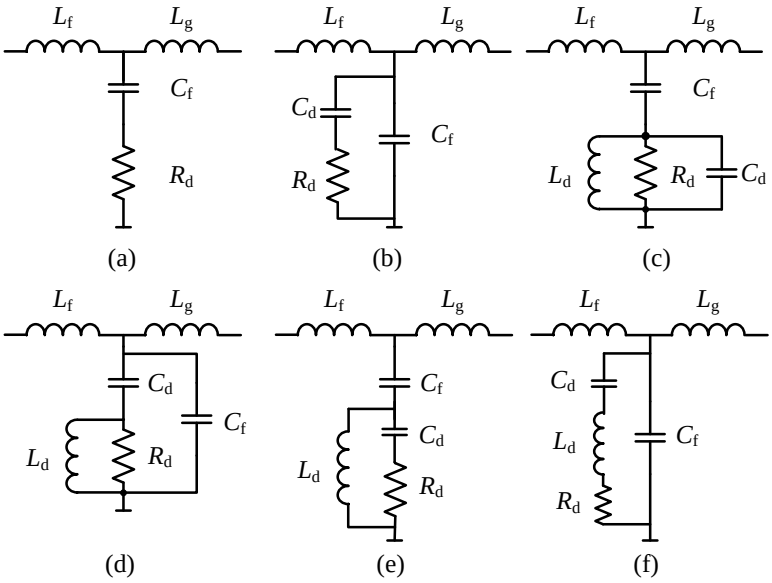

Figure 1-12. Configurations of passive damping resistor, (a) series R damper, (b) shunt RC damper, (c) series RLC damper, (d)shunt RLC damper, (e) third order damper, (f) single tuned damper.

3) Active Damping of Grid-Connected VSIs. In order to avoid the power loss introduced by the damping resistor, various active damping methods have been proposed [94], [103]–[105]. Most active damping methods introduce additional feedback signal to dampen the resonance peak of the LCL filter, the signals used in the literatures include:

- Capacitor current feedback [104];
- Capacitor voltage feedback [106]–[108].

Modification of the current reference and grid voltage feedforward can also be applied to stabilize the VSI. Since the time delay of the PWM process may lead to the phase crossing of -180 degrees of the open loop gain, delay compensation is also investigated to improve the stability of the VSIs [109]–[111]. Even though the active damping method is effective for single VSI for inductive grid impedance, the effectiveness of them are corrupted when multiple VSIs are paralleled. Also, for high power VSI with low switching frequency, the active damping method may not be effective due to the limited control bandwidth [30].

4) Active Damper for PE based Power System. The active damper has recently been proposed to stabilize the PE based power system [33], [112]–[115]. The topologies of the L filtered and LC filtered active damper are shown in Figure 1-13. It re-shapes the grid impedance seen by each VSI by mimicking the behavior of a damping resistor, thus it is more effective and reliable for complex grid conditions. Unlike the traditional R-APF, the active damper suppresses the harmonic resonance caused by the interactions among the VSIs, which has much higher order and varies in a wide frequency range [33]. Proportional and Resonant (PR) controller has been used to control the output current of the active damper at the harmonic resonance frequency.

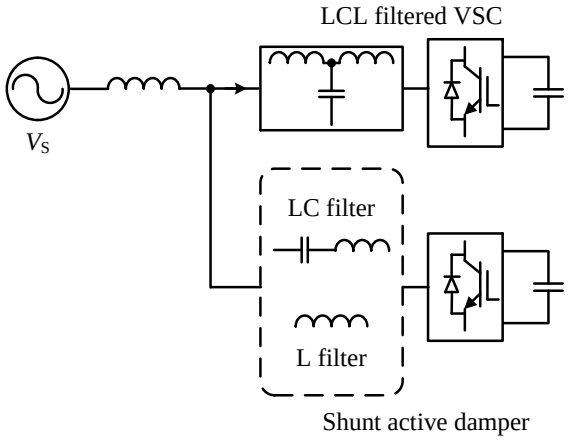

Figure 1-13. Topology of active damper configurations.

Since the resonance frequency is unknown and may not be integer times of the fundamental frequency, online frequency detection is needed and has been proposed [113]. Nevertheless, the real-time resonance frequency detection is challenging and remains to be further improved.

1.3. APPLICATION OF SERIES-LC FILTERED VSI IN PE BASED POWER SYSTEMS

As mentioned above, the APF technologies have been used to mitigate all the harmonics appearing in a PE based power system, except for the near-synchronous resonance. Compared with the traditional L or LCL filtered APFs, the HAPFs shown in Figure 1-6 have some proven advantages, such as reduced power rating of the VSI and system cost. Furthermore, the type I HAPF, or the series LC filtered VSI, has been reported in several literatures to provide the resonance damping and harmonic filtering service for the grid [80], [84]-[86], [112], [116]. Also, the current flowing into the HAPF can be directly controlled by the VSI. In this section, the application of the series LC filtered VSI is briefly reviewed.

1.3.1. RESONANCE DAMPING FOR PASSIVE POWER FILTERS

In [80], [116], the Passive Power Filters (PPFs) tuned at the dominating harmonics are utilized as the series LC filter for the HAPF, while the capacitor is designed to provide the desired reactive power compensation. The typical topology of the system is shown in Figure 1-14. Due to the existence of capacitive components, harmonic resonance can be introduced which may cause overcurrent and overheating of the PPFs. The VSI is used to emulate a damping resistor to dampen the harmonic resonance and protect the passive filters from overheating and overcurrent. The control circuit of the HAPF is shown in Figure 1-15(a). The harmonic component of the source current i_S or the filter current i_F is extracted and multiplied by the control

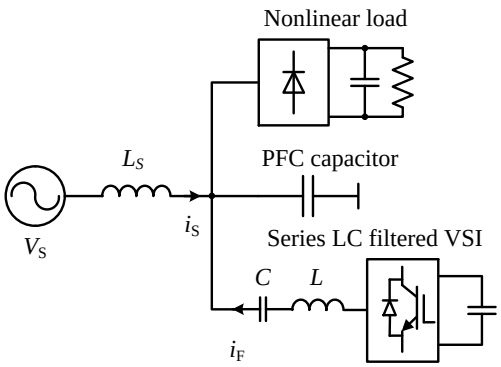

Figure 1-14. Network model of system equipped with nonlinear load and series LC filtered VSI.

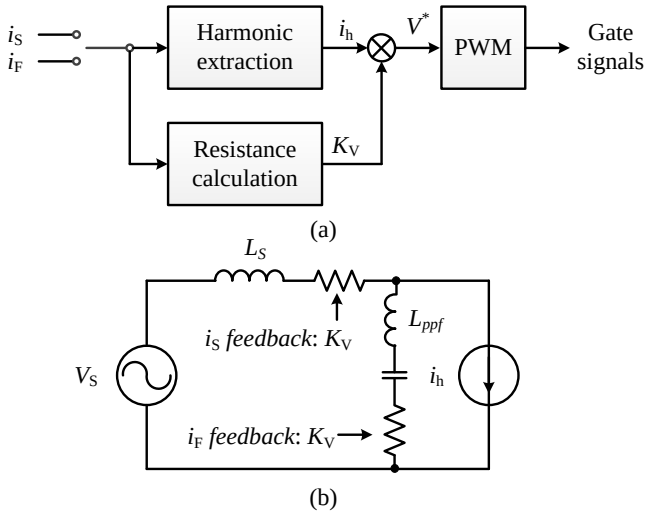

Figure 1-15. Control circuit of the HAPF and equivalent model, (a) control circuit, (b) equivalent model.

gain K_v to form the voltage reference. Since the LC filter is tuned at the dominating harmonics (often the 5^{th} harmonic), the VSI can then be regarded as a damping resistor with K_v ohm.

The equivalent circuit of the system in Fig. 1-14 is shown in Figure 1-15(b). For the filter current i_F feedback, the virtual resistance is connected in series with the LC filter. For the source current i_S feedback, the virtual resistance is connected in series with the grid impedance. With the virtual resistance, harmonic resonance at the the 5^{th} can be effectively dampened. The virtual resistance K_v can be adjusted online based on the amplitude of the 5^{th} order harmonic.

1.3.2. SERIES LC FILTERED R-APF

The HAPF can also be controlled as the R-APF, where the VSI and the series LC filters can be viewed as a resistor together. The control structure of the series LC filtered R-APF is shown in Figure 1-16. Like the traditional R-APFs, the voltage at the PCC is measured to generate the current reference. Different control targets can be achieved by changing the current reference of the R-APF. A current controller is used to track the reference and online adjustment of the virtual resistance can be achieved by comparing the THD of the voltage to a given value [80]-[82]. In order to achieve unity closed-loop gain, paralleled Resonant (R) controllers tuned at the harmonics are used to increase the open loop gain of the current control loop. Due to the high open loop gain, the PCC voltage has little influence on the output current.

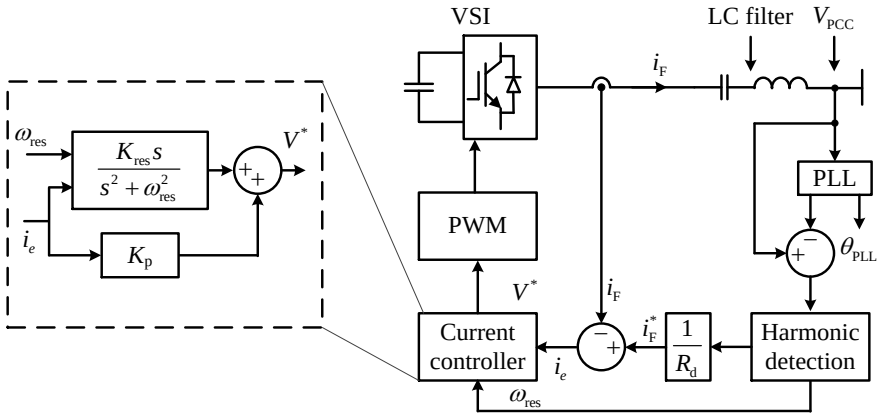

Figure 1-16. Control structure of the series LC filtered active damper as an R-APF.

The series LC filtered VSI can also be used to suppress the harmonic resonance caused by the instability issue, which is denoted as the "active damper" (active stabilizer) in some literatures [113], [117]. The control system of the active damper is similar with that of an R-APF. However, online resonance frequency detection is needed to tune the resonant part of the current controller [113]. Even though various frequency detection algorithms have been proposed, they increase the computational burden of the control system greatly, which confines the real applications of the active dampers.

1.4. PROJECT MOTIVATION

1.4.1. PROBLEM STATEMENT

In present researches on the control of the series LC filtered VSIs, either the VSI emulates the virtual resistance (Figure 1-14) or the whole HAPF emulates the resistance (Figure 1-16). For the PE based power system, the latter one is better since it offers more controllability at the system level. Research on using the series LC filtered VSI to mitigate the switching harmonics of a high power VSI has not been reported.

For the series LC filtered R-APF and the active damper, the VSI is controlled to be a current source. Even though the reference current is dependent on the harmonic component of the PCC voltage, the influence of the PCC voltage as a disturbance for the current control loop of the APF is neglected. However, given the wide frequency range of the harmonics in a PE based power system, the targeted frequencies for the APFs can be both unknown and too high for the APFs to track. To be more specific, there are following challenges for the application of series LC filtered VSIs.

- For the active dampers, the emulation of damping resistance at unknown frequencies is challenging. The frequencies of the harmonic resonance can be inter-harmonics. Without the knowledge the resonance frequency, it is difficult to tune the resonant controllers and achieve unity closed-loop gain for the current control loop.
- For the APFs used to mitigate the switching frequency of a high power VSI, the targeted frequencies are at kilo Hertz level and are much higher than the normal APFs intended for the LCC-originated harmonics. The current control at those frequencies is not trivial since they are above the normal control bandwidth of VSIs switching which is below 20 kHz.

1.4.2. IMPEDANCE MODEL OF SERIES LC FILTERED VSI

For the current controlled VSIs, the Norton equivalent model is shown in Figure 1-17. In the figure, the current source I_S represents the current introduced by the current reference and the closed-loop system. The output admittance Y_o reflects the influence of the disturbance on the final output current. Usually, the output admittance is very low and can be neglected. As a result, in most existing researches, the current controlled APFs are represented by a current source. The impedance model of LC filtered VSI has not received much attention, while the impedance model of the LCL filtered grid-connected VSIs has been studied intensively [58]-[62].

Meanwhile, in the output admittance, the current controller of the VSI can be represented physically. The proportional controller introduces a virtual resistance and the integral or resonant controller introduces a virtual capacitance in the Norton equivalent model. With the physical representation of the current controllers, the output admittance of the APFs may bring new possibilities for the control system design of the series LC filtered VSIs. Apparently, the following hypothesizes can be established:

- The virtual resistance introduced by proportional controller of the active damper can provide the damping resistance for the PE based power system;
- With the passive LC filter and the virtual impedance introduced by the current controller, various impedances can be synthesized by the series LC filtered VSI without any accurate current reference tracking.

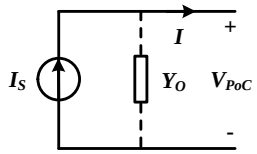

Figure 1-17. Norton equivalent model of the current controlled VSI.

1.4.3. PROJECT MOTIVATION

As discussed above, the accurate current reference tracking is the obstacle for the application of the series LC filtered VSI for resonance damping at unknown frequencies and switching harmonic attenuation for the high power VSIs. Meanwhile, it is possible to use the output admittance of the series LC filtered VSI for the harmonic damping and mitigation in a PE based power system, as hypothesized above. As a result, this thesis is motivated to explore the possibilities of using the output admittance of the current controlled series LC filtered VSI to mitigate the harmonics and reduce instability.

1.5. RESEARCH OBJECTIVES

In this thesis, the impedance model of current controlled VSIs including the normal LCL filtered grid-connected inverter and the series LC filtered VSI are first investigated. The objective is to develop the control strategies of the series LC filtered VSI to achieve the following targets based on the impedance model:

1) Harmonic stabilization in PE based power system;
2) Integration of series LC filtered VSI to high power VSI to improve the output current quality;
3) Damping of the LCC-originated harmonics in the PE based power system.

1.5.1. HARMONIC STABILIZATION OF PE BASED POWER SYSTEM

In order to study the harmonic stabilization of the PE based power system using the series LC filtered VSI, the following research targets are covered:

- Review of the existing research on the stability analysis and enhancement methods for grid-connected VSIs with LCL filter;
- Investigation on the mechanism on how the series LC filtered active damper stabilizes the harmonic instability of PE based system;
- Simplification of the control system of the active damper based on the developed impedance model.

In the research on IBS analysis of grid connected VSIs, the concept of passivity will also be applied [60]-[62]. If the output admittance of a VSI is passive in a frequency range, it means the current control loop is stable under ideal grid voltage and it can dissipate energy in the passive frequency range. As long as the real part of the output admittance of the series LC filtered active damper is positive, the active damper can always provide damping for the system.

The control target of the series LC filtered active damper in this thesis is changed from mimicking the behavior of resistor to enhancing the passivity of the PE based

system. The real part of the output admittance of the active damper with only a proportional current controller is investigated. As a result, the online detection of the resonance frequency is not needed for the active damper.

1.5.2. INTEGRATION OF SERIES LC FILTERED VSI WITH HIGH POWER VSI

The detailed research objectives in this part include the following:

- Switching harmonic attenuation of switching harmonics of high power VSI based on series LC filtered VSI;
- Low order harmonic distribution analysis and mitigation of the high power VSI based on series LC filtered VSI.

The limitation of the conventional VSI-based APF in the switching harmonic attenuation of a high power VSI is mainly the current control at high frequency. Instead of tracking certain current reference, this thesis explores the possibility to use the series LC filtered VSI to provide low impedance path to bypass the switching ripples of a high power VSI. Based on the output impedance of the series LC filtered VSI, the low impedance path can be synthesized with a special current controller, while the current reference can be set to zero.

In order to develop proper control system of the series LC filtered VSI, the impedance model of the system with a high power VSI and the series LC filtered VSI will be investigated at the low order harmonics. Note that two impedance models are needed to describe the system since at two different frequency ranges. At the switching frequency of the high power VSI, it can not be modelled using the impedance based method since it is above its Nyquist frequency. At the low order harmonics, both the high power VSI and the series LC filtered VSI can be modeled using the IBS method. The operation principles can then be derived based on the two impedance models.

1.5.3. DAMPING OF THE LCC-ORIGINATED HARMONICS IN PE BASED POWER SYSTEM

For the series LC filtered R-APF, the output impedance of the VSI will be investigated to provide the desired virtual resistance at the harmonic frequencies. Since the output impedance is independent on the current reference, the harmonic grid voltage is not measured for the reference generation. However, the grid voltage needs to be measured for synchronization, which is necessary for the dc-link voltage control. Hence, the elimination of the AC side voltage sensor can only be expected if the dc-link control can be carried out without any AC voltage sensor. In this part of the research, there are two specific goals:

- Virtual resistance synthetization with the output impedance of the series LC filtered VSI;
- AC voltage sensorless control of the dc-link voltage.

1.6. THESIS OUTLINE

This thesis starts with the harmonic stablization of the PE based power system using the series LC fitlered VSI in *Chapter 2* and *Chapter 3*. Impedance Based Stability (IBS) analysis of the normal grid-connected LCL filtered VSIs and the corresponding experimental verification are carried out in *Chapter 2*. Next, the IBS is carried out for the series LC filtered VSI in *Chapter 3*, where the system stablility is impoved by controlling the LC filtered VSI as the "active damper" [119]. Investigation on the mechanism on how the series LC filtered active damper stabilizes the PE based system is carried out in this paper. Also, the control system of the active damper is simplified based on the developed impedance model.

Next, the impedance model of the series LC filtered VSI is further utilized for switching harmonic attenuation in *Chapter 4*. The "active trap filter" is proposed in this chapter, which is effective at by-passing the switching harmonics of the high power VSI with low switching frequencies [120]. *Chapter 5* continues the work on the active trap filter and analyses the low order harmonic distribution within the system of a high power VSI and the active trap filter. Control strategy is developed so that the active trap filter can mitigate also the low order harmonics introduced by the background distortion in the grid [121].

In *Chapter 6*, the control strategy of the series LC filtered VSI is proposed to dampen the LCC-originated harmonics. The impedance model of the series LC filtered VSI is utilzed again to emulate damping resistance at the low order harmonics, enabling the voltage sensorless Resistive-APF (R-APF) [122].

Finally, *Chapter 7* summarizes the main conclusions ans points out the future works of this thesis. Each chapter from *Chapter 2* to *6* is composed of a journal paper. The short introductions from *Chapters 2* to *6* are listed below:

Chapter 2 gives the first paper, published in the *IEEE Transactions on Industrial Applications*. In this paper, the IBS analysis is first carried out for a renewable energy power plant with multiple LCL filtered VSIs. The non-passive frequency ranges of the output admittance of the VSIs are calculated. It is shown that the non-passive frequency range is related to the LCL parameter, control strategy and the time delay in the current control loop. Analytical expressions of the non-passive frequency region are derived. Then, a passivity enhancement method is proposed. Instead of using VSIs with the same parameter, this paper suggests to adopt VSIs with different LCL parameters, control strategies and sampling frequencies, which are dependent on the power rating. In such a way, the negative-real part of the output

admittance will be cancelled among the VSIs. The power plant as well as individual VSI will remain stable with both inductive and capacitive grid impedance.

Chapter 3 gives the second paper, published in the *IEEE Transactions on Industrial Electronics*. In this paper, the Norton equivalent circuit of the series LC filtered active damper is developed, which consists of a current source and an output admittance. The output admittance has been neglected in many literatures, but it is investigated in this paper. By controlling the current source as a virtual resistor, the current source can be viewed as an additional admittance connected in parallel with the output admittance of the active damper. The proportional current control is used for the active damper and the online detection of the resonance frequency is not needed. It is shown that above the current control bandwidth, the additional admittance introduced by the current source will have a negative real part, which corrupts the stability of the system. To solve this problem, a low-pass filter is connected in series with the current controller. The resultant total output admittance of the active damper becomes passive in a wide frequency range.

Chapter 4 gives the third paper, published in the *IEEE Transactions on Power Electronics*. In this paper, an Active Trap Filter (ATF) based on the series LC filtered VSI is proposed to attenuate the switching harmonics of a high power VSI with low pulse ratio. The sideband frequencies of the switching harmonics of the high power VSI can be up to several kilo Hertz. The current control at this frequency level with limited switching frequency (below 20 kHz) is challenging. The operation principle of the ATF is to provide zero output impedance at the sideband frequencies of the high power VSI. In such a way, the ATF can be viewed as a current-controlled voltage source and the current reference can simply be set to zero. The performance of the ATF is not dependent on the current control bandwidth, thus the normal IGBT with an operation frequency below 20 kHz can be used. The impedance model of the grid-connected VSI has been studied intensively for the IBS analysis. It is the contribution of this paper to use the impedance model for harmonic attenuation.

Chapter 5 gives the fourth paper, submitted to the *IEEE Journal of Emerging and Selected Topics on Power Electronics*. Due to the low control bandwidth of high power VSIs, the background harmonic in the grid voltage causes the distortion of the output current on the high power VSI. In this paper, both the switching harmonics and the low order harmonics in the output current of a high power VSI is compensated with the series LC filtered VSI, whose power rating is low. The operation principle of the low power VSI is obtained by the impedance model of the system. At the low order harmonics, the low power VSI acts as a current source controlled by the converter side current of the high power VSI. At the swtching harmonics, the low power VSI should provide zero output impedance. A modified PR controller is used as the current controller of the low power VSI.

Chapter 6 gives the fifth paper, accepted by the *IEEE Transactions on Power Electronics*, where a AC voltage sensorless R-APF is proposed. Unlike the traditional R-APF, which controls its output current to track the reference that is obtained with the harmonc voltage information, the output impedance of the proposed R-APF emulates a damping resistor. The current reference is set to zero and the current controller is composed of proportional controller and paralleled Quadrature Signal Generators (QSGs). What is more, for the dc-link voltage control, the traditional control method needs to measure the grid voltage for the purpose of synchronization. In this paper, a grid voltage estimation method is proposed to obtain the fundamental component of the grid votlage. Hence, the AC voltage sensor can be removed, which not only reduces the system cost but also improves the isolation between the control loop and the power loop of the R-APFs.

CHAPTER 2.

Paper 1

Passivity Enhancement in RES Based Power Plant with Paralleled Grid-Connected Inverter

Haofeng Bai, Xiongfei Wang, Frede Blaabjerg

The paper has been accepted by
IEEE Transactions on Industrial Applications
vol. 53, no. 4, 3793-3802, July-Aug. 2017.
DOI 10.1109/TIA.2017.2685363

2.1. BRIEF SUMMARY

Nowadays, more and more Renewable Energy Source (RES) based power plants are being installed in the power systems, where multiple LCL filtered grid connected inverters are connected to the same Point of Common Coupling (PCC) [1]-[3]. The grid impedance between the PCC and the voltage feeder or the ideal voltage source can either be inductive or be capacitive. The typical topology of such a power plant is shown in Figure 2-1. In order to increase the power capability of the power plant, more inverters should be paralleled. However, the number of the inverters is sometimes limited by the stability issues since the equivalent grid impedance seen by each inverter increases with the number of paralleled inverters [26].

In this paper, the stability of RES based power plant with multiple grid-connected converters is first analyzed using the impedance based technique. The impedance model of the system shown in Figure 2-1 is drawn in Figure 2-2, where each inverter is represented by its Norton equivalent model. Based on the model, the total current I_{g_t} and the output current of the i^{th} inverter I_{g_i} can be obtained as [118]

$$I_{g\_t} = I_{S\_t}\frac{1}{1+T_m} - \frac{V_S}{Z_S}\frac{T_m}{1+T_m} \tag{2.1}$$

$$I_{g\_i} = I_{S\_i}\left(1-\frac{T_{m\_i}}{1+T_m}\right) - \left(I_{S\_t} - I_{S\_i}\right)\frac{V_S}{Z_S}\frac{T_{m\_i}}{1+T_m} - \left(\frac{V_S}{Z_S}\right)\frac{T_{m\_i}}{1+T_m} \tag{2.2}$$

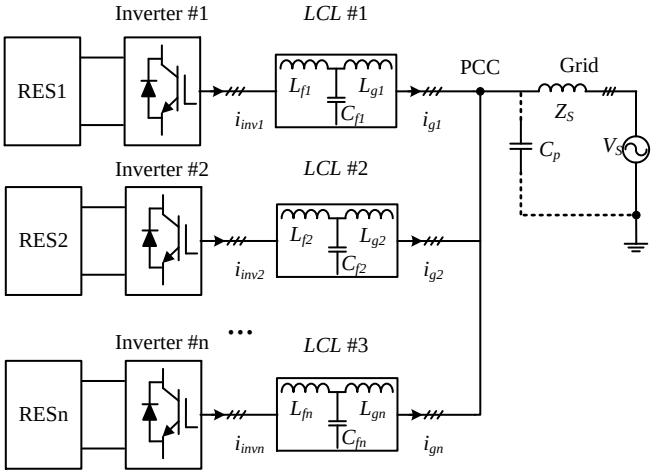

Figure 2-1. Topology of the RES based power plant with multiple grid-connected inverters in parallel, quoted from [118].

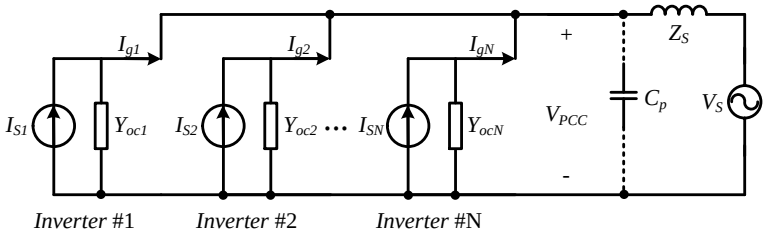

Figure 2-2. Impedance model of RES based power plant, quoted from [118].

where

$$T_m = \frac{Y_{oc\_t}}{Y_{cp} + Y_S} \tag{2.3}$$

and

$$T_{m\_i} = \frac{Y_{oc\_i}}{Y_{cp} + Y_S} \tag{2.4}$$

are the admittance ratio between the total output admittance of the power plant Y_{oct} and the grid admittance and the i^{th} output admittance Y_{oci} and the grid admittance. The system stability can be judged by the admittance ratio T_m through the Nyquist criterion [5]. Next, the passivity or net damping of the whole system is investigated regarding the parameters of each individual inverter. The passivity is a desired property of the impedance model of the inverters. If the inverter is passive, it means that the real part of its output admittance is positive and it contributes to the net damping of the whole system [22]. If each inverter is passive, then the system will be stable. However, due to the time delay in the current control loop, the non-passive frequency ranges are introduced, where the real part becomes negative. The non-passive frequency ranges have been calculated for both the grid and inverter current controlled inverters. The results are shown in Table 2.1. In the table, f_{LC} is the resonance frequency of the inverter side LC filter, and f_s is the sampling frequency. From the table, it can be seen that the non-passive range is dependent on both the LCL filter and the sampling frequency used.

Table 2.1 Non-Passive Frequency Regions for the LCL Filtered Inverters, quoted from [118]

Controlled Current	Position of f_{LC}	Non-Passive Region
Inverter Side Current	-	$[f_s/2, f_s/6]$
Grid Side Current	$f_{LC} > f_s/6$	$[f_s/6, f_{LC}]$
	$f_{LC} < f_s/6$	$[f_{LC}, f_s/6]$

Then the paper proposes to use inverters with different LCL filters and sampling frequencies to cancel the negative real parts in the frequency domain. This suggests the system designer of the power plant to adopt inverters with different parameters in order to improve the system stability. Three cases where two different inverters are paralleled are studied in this paper: case 1), inverter side current control & grid side current control; case 2), grid side current control with different f_{LC}; and case 3), grid side current control with different sampling frequencies. Both simulation and experimental results are obtained to support the effectiveness of the proposed method. The Nyquist plots of the admittance ratio T_m in the three cases are shown in Figure 2-3, where the encirclement of the critical point can be found with only one type of inverter and no encirclement can be observed with two types of inverters. The corresponding experimental results are shown in Figure 2-4. The results show that with only one type of inverter, the system is unstable; when two different inverters are connected, the system becomes stabilized.

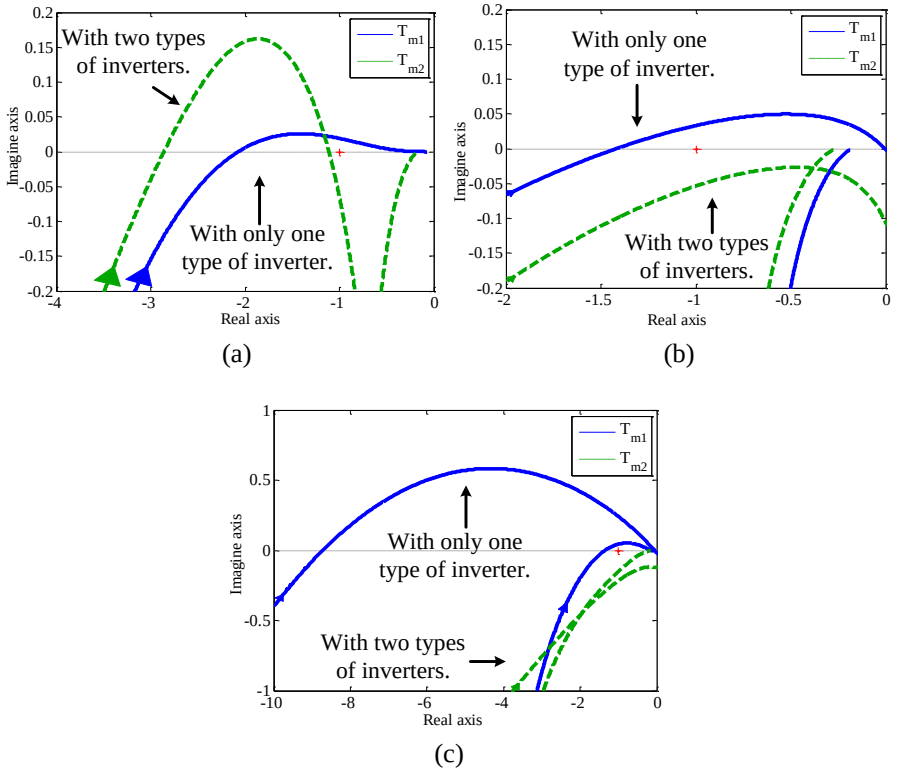

Figure 2-3. Nyquist plot of the admittance ratio in the three cases, quoted from [118]. (a) case 1, (b) case 2, and (c) case 3.

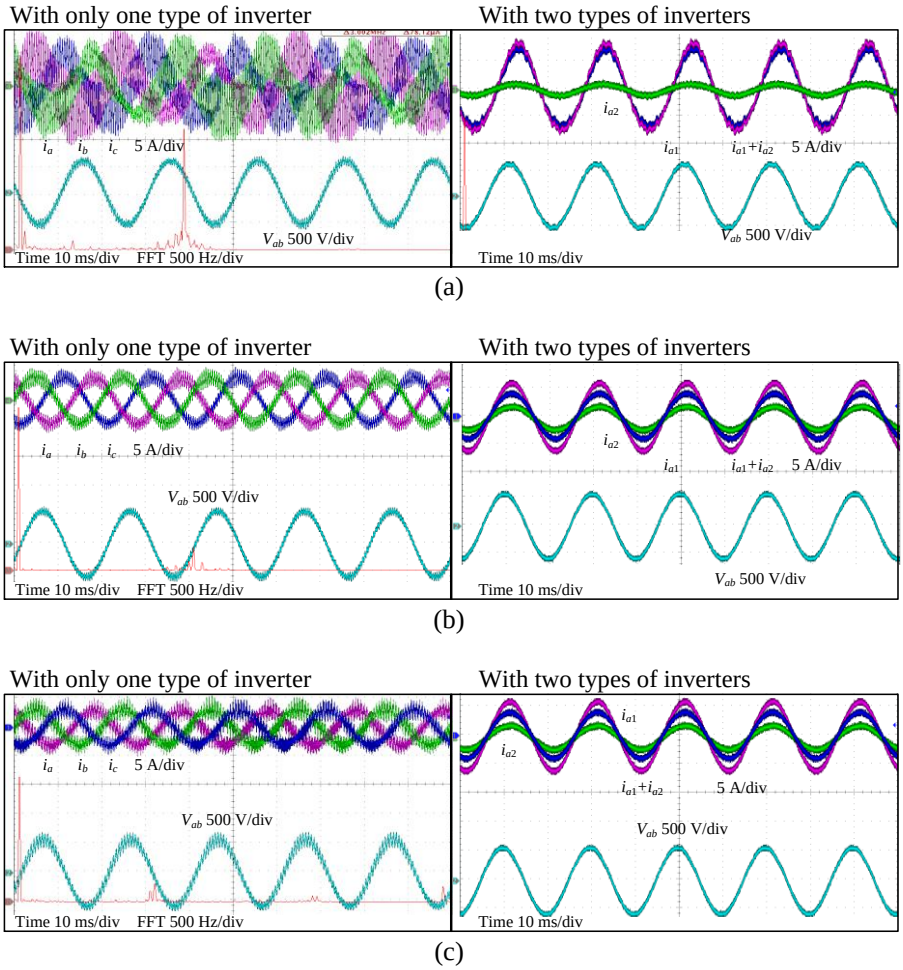

Figure 2-4. Experimental results in the three cases, quoted from [118]. (a) case 1, (b) case 2, and (c) case 3.

2.2. KEY CONTRIBUTIONS

There are mainly two contributions in this chapter. First, the impedance based stability analysis method is experimentally verified. The impact of the grid inductance has been studied in many literatures, while the grid capacitance is seldom considered. In this chapter, the impact of the grid capacitance is also analyzed. Secondly, the passivity enhancement method is proposed and experimentally verified. The proposed method does not require any additional sensors as required in many active damping methods.

The contributions of this chapter lie the foundation to achieve research objective 1) in *Chapter 1. 5*. Even though the active damper is not considered, it is shown in this chapter that enhancing the passivity can be the operation target for the active damper.

CHAPTER 3.

Paper 2

Passivity Enhancement of Grid-Tied Converters by Series LC-Filtered Active Damper

Haofeng Bai, Xiongfei Wang, Poh Chiang Loh, Frede Blaabjerg

The paper has been published in
IEEE Transactions on Industrial Electronics
vol. 64, no. 1, pp. 369-379, Jan. 2017.
DOI: 10.1109/TIE.2016.2562604

3.1. BRIEF SUMMARY

In this paper, the stability of grid connected inverters with LCL filters is improved using the series LC filtered active damper. The topology of the system studied in this paper is shown in Figure 3-1, quoted from [119]. In the figure, there is an LCL filtered Voltage Source Inverter (VSI) and an active damper composed of a series LC filter and a low power VSI. Since the series capacitor sustains the fundamental voltage, the required dc-link voltage of the active damper is greatly reduced. In previous studies, the active damper is controlled to mimic the behavior of a damping resistor, which is done by using a current controller tuned at resonance frequency in the system and neglecting the output admittance of the active damper itself [33]. However, the online detection of the resonance frequency and the tuning of the damping effort remain open issues [113].

The tuning method of the damping effort for the active damping is proposed and output admittance of the active damper itself is analyzed in this paper. First, the Norton equivalent circuits of the LCL filtered VSI is built, which is shown in Figure 3-2(a) [119]. In the figure, i_{INV}^{*} is the current reference, G_{cl} is the closed-loop gain of the current control loop and Y_{oc} is the output admittance. The grid impedance is L_s and R_s. The minimum value of the real part of the output admittance of the LCL filtered VSI Y_{oc} is estimated with the largest magnitude of Y_{oc} at 1/6 of the sampling frequency assuming that Y_{oc} is pure real part. In fact this estimated damping effort is larger than the needed value since there is always an imaginary part in Y_{oc}. The estimated value is then set to be the resistance that the active damper needs to mimic.

Next, the impedance model of the active damper itself is built using the same method, which is shown in Figure 3-2(b). Since the current reference of the active damper is obtained by dividing the harmonic voltage with the damping resistance, the current source in the Norton equivalent circuit can be replaced with a virtual admittance. Hence, the total damping effort of the active damper comes not only from tracking the current reference but also from its own output admittance.

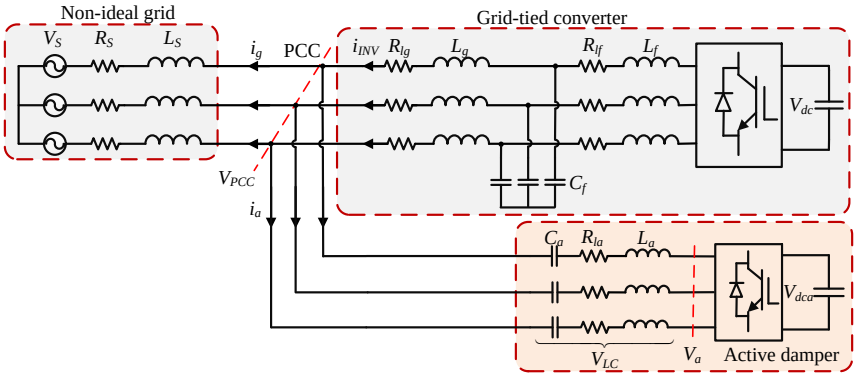

Figure 3-1. System topology studied, quoted from [119].

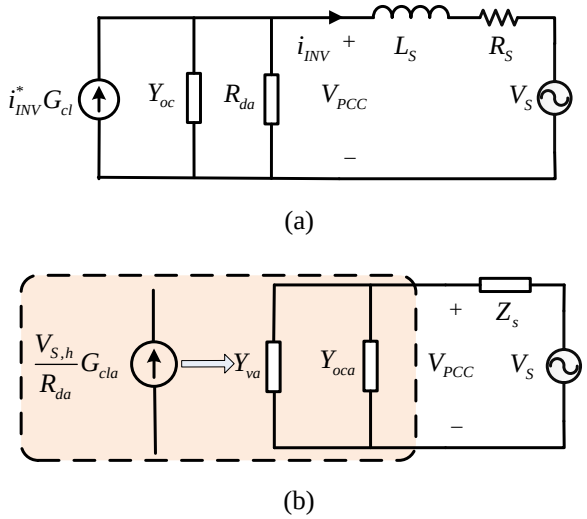

Figure 3-2. Impedance model of the LCL filtered VSI and the active damper, quoted from [119]. (a) LCL filtered VSI, and (b) active damper.

In order to avoid the online detection of the resonance frequency, only the proportional controller is used as the current controller of the active damper. Without the resonant controller, there is no need to detect the resonance frequency while the open loop gain is not high at the resonance frequency. Hence the control bandwidth is limited. This imperfection of the closed-loop control introduces additional negative real part for the active damper. A simple first order low-pass filter is used to solve this problem and the impact of the closed-loop control is minimized above the control bandwidth. The resultant current control loop of the active damper is shown in Figure 3-3. In order to show the performance of the

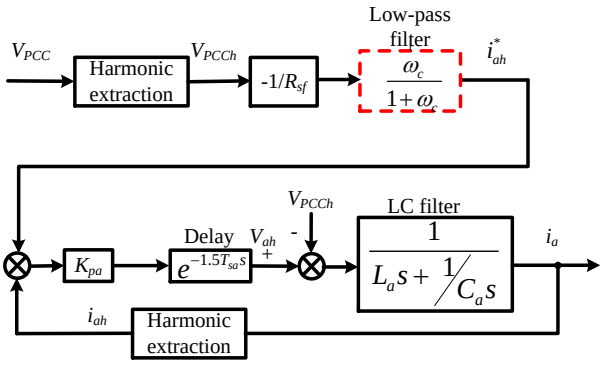

Figure 3-3. Proposed current control loop with output admittance shaping, quoted from [119].

Table 3.1 Parameters of the Grid Converter, quoted form [119]

	Parameter	Value
Electrical parameters	L_{fc}	4.9 mH
	R_{lf}	0.2 Ω
	C_f	10 µF
	L_{fg}	1.8 mH
	R_{lg}	0.2 Ω
	f_{LC}	718 Hz
Control parameters	f_s	5 kHz
	T_s	200 µS
	K_p	20

Table 3.2 Parameters of the Active Damper, quoted from [119]

	Parameter	Value
Electrical parameters	L_a	1.8 mH
	C_a	10 µF
	R_{la}	0.1 Ω
	V_{PCC} (RMS)	230 V
Control parameters	f_{sa}	10 kHz
	T_{sa}	100 µS
	K_{pa}	4
	K_{pa_dc}	10
	K_{ia_dc}	0.5

proposed control method of the active damper, simulation and experiments are carried out with the parameters listed in Table 3.1 and Table 3.2, respectively. The Bode plots of the total admittance seen by the grid with / without the output admittance shaping method are shown in Figure 3-4(a) and (b), respectively.

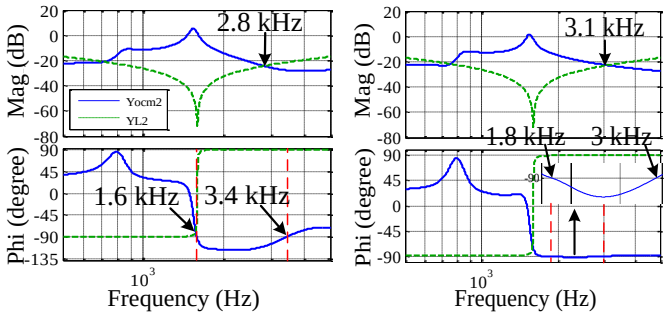

(a) (b)

Figure 3-4. Bode plots of the admittance seen by the grid, quoted from [119]. (a) without output admittance shaping, and (b) with output admittance shaping method.

As it can be seen from Figure 3-4, without the low-pass filter, there is a non-passive region between 1.6 kHz and 3.4 kHz. The system is robust to inductive grid impedance but harmonic instability can be introduced by capacitive grid impedance. With the low-pass filter, the non-passive region is almost eliminated. The enhanced passivity improves the stability of the system regardless of the grid impedance.

In the experiment, the system is first exposed to inductive grid impedance of 2.7 mH. The PCC voltage and grid current are unstable without the active damper, as is shown in Figure 3-5(a). When the active damper without the output admittance shaping method is connected, the system is stabilized as shown in Figure 3-5(b). When the grid impedance becomes capacitive, the system becomes unstable even with the active damper, as is shown in Figure 3-5(c). After enabling the output admittance shaping of the active damper, the system is stabilized, as it is shown in Figure 3-5(d).

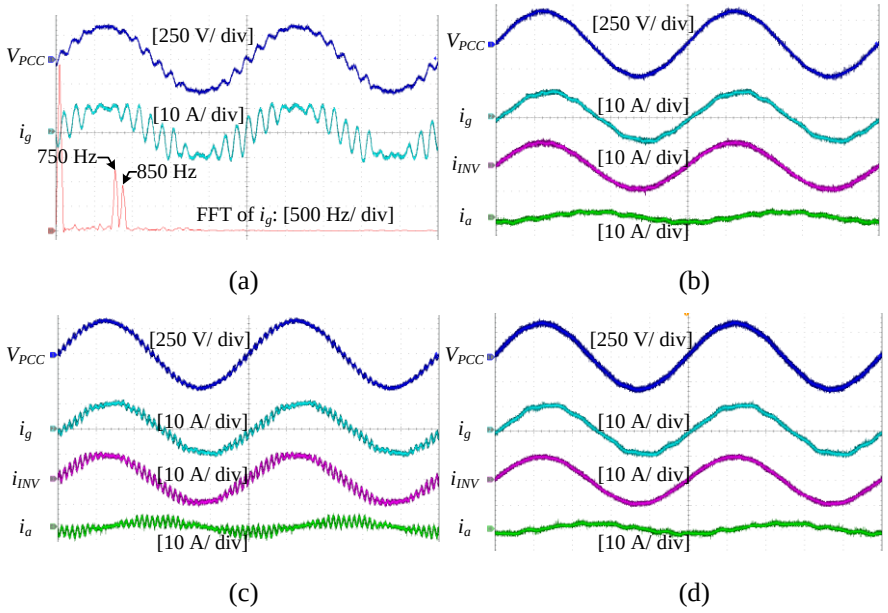

Figure 3-5. Key experimental results, quoted from [119]. (a) harmonic instability of the LCL filtered VSI against inductive grid impedance, (b) stabilized system with active damper against inductive grid impedance, (c) harmonic instability against capacitive grid impedance without output admittance shaping method, and (d) stabilized system against capacitive grid impedance with the output admittance shaping method.

3.2. KEY CONTRIBUTIONS

There are mainly two contributions in this chapter. First, the tuning method for the damping resistance of the active damper is proposed. The idea is to guarantee the passivity of the system with the active damper. The largest magnitude of the output admittance of the LCL filtered VSIs is chosen as the virtual damping resistance, which appears at 1/6 of the sampling frequency. Second, the current control loop of the active damper is simplified with a proportional current controller and a low-pass filter. With the low-pass filter, the output admittance of the active damper is re-shaped above its current control bandwidth and the system is robust to both inductive and capacitive grid impedance.

The contributions of this chapter achieve research objective 1) of using the series LC filtered VSI to stabilize the PE based power system. The working mechanism of the active damper is investigated and the control strategy is simplified.

CHAPTER 4.

Paper 3

An Active Trap Filter for Switching Harmonics Attenuation of Low-Pulse-Ratio Inverters

Haofeng Bai, Xiongfei Wang, Poh Chiang Loh, Frede Blaabjerg

The paper has been accepted by
IEEE Transactions on Power Electronics
DOI: 10.1109/TPEL.2017.2657644

4.1. BRIEF SUMMARY

The switching harmonics attenuation is challenging for the high power Voltage Source Inverters (VSIs) with low switching frequencies [45], [48]. In this paper, an Active Trap Filter (ATF) is proposed based on the physical interpretation of the current controllers in its impedance model. The topology of the studied system is shown in Figure 4-1. In the figure, the ATF is composed of a series LC filter and a low power VSI and it is connected to the middle point between the inverter side and grid side inductors of the main VSI. The operation principle of the ATF is to provide a zero impedance path at the switching frequencies of the main VSI and the switching harmonics can be bypassed by the ATF. The unique feature of the ATF is that its impedance characteristic is achieved not by tracking certain current reference, but by utilizing the output impedance of the ATF itself.

In order to understand the physical meaning of the current controllers in the impedance model, the current control loop and the Thevenin equivalent circuit of a normal L filtered VSI are shown in Figure 4-2(a) and (b), respectively. Based on Figure 4-2(a), the output current I can be obtained as

$$I = \underbrace{G_{cl}(s) I_{ref}}_{\text{Current Source } I_S} - \underbrace{\frac{Y_L(s)}{1+T_o(s)}}_{\text{Output Admittance } Y_o} V_{PoC}, \tag{4.1}$$

where

$$G_{cl}(s) = \frac{T_o(s)}{1+T_o(s)},$$

$$T_o(s) = Y_L(s) G_{cc}(s) G_d(s).$$

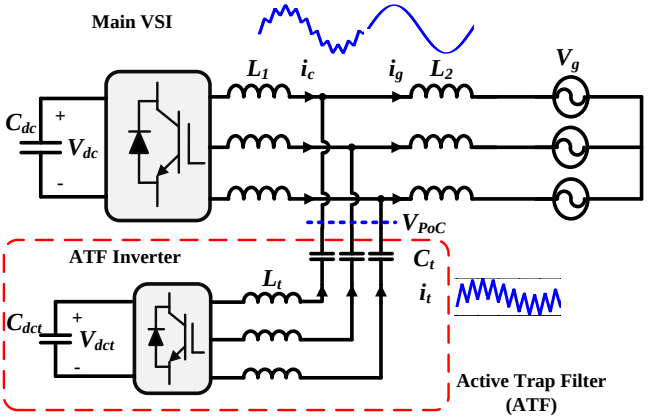

Figure 4-1. Topology of the high power voltage source inverter with the proposed active trap filter to reduced switching harmonics, quoted from [120].

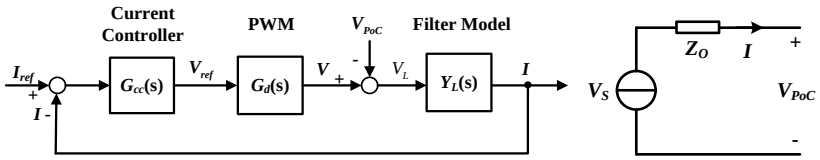

(a) (b)

Figure 4-2. Impedance model of L filtered VSI, quoted from [120] (a) current control loop, and (b)) Thevenin equivalent circuit.

Equation (4.1) leads to the impedance model shown in Figure 4-2(b), where the voltage source V_S and the output impedance Z_o can be calculated as

$$V_S = \frac{I_S}{Y_o} = G_{cc}(s) G_d(s) I_{ref} \tag{4.2}$$

$$Z_O(s) = \frac{1}{Y_L(s)} + G_{cc}(s) G_d(s) = Z_L(s) + Z_{CC}(s) \tag{4.3}$$

If the time delay in the power converter G_d(s) is neglected in (4.3), the impacts of the current controller on Z_O are clear:

- The Proportional (P) controller will introduce a virtual resistance.
- The Integral (I) controller under rotating dq-frame and the Resonant (R) controller under the stationary frame will introduce a virtual capacitance.

It should be noted that the integral or resonant controller has a phase shift of 90 degrees above the resonance frequency, which is the origin of the capacitive output impedance. In this paper, the Quadrature Signal Generator (QSG) is used as the current controller due to its frequency characteristic of 90 degree's phase shift and unit gain at the resonance frequency. Considering the time delay G_d(s), the QSG should compensate the additional phase lag introduced by G_d(s) at the resonance frequency. Instead of the standard QSG, the following modified QSG with phase compensation can be used.

$$G_{QSGm}(s) = \frac{2\omega_c \sin(\alpha) s + 2\omega_c \omega_t \cos(\alpha)}{s^2 + 2\omega_c s + \omega_t^2} \tag{4.4}$$

where α is the compensated phase lag.

$$\alpha = 1.5\omega T_s \tag{4.5}$$

With the modified QSG, the output impedance of the ATF can be calculated as

$$Z_{oca}(s) = Z_{LC}(s) + G_d(s)\sum_{i=1}^{N} K_i G_{QSGm\_i}(s) \tag{4.6}$$

Thus, the virtual capacitance can be introduced at the resonance frequency. With the virtual capacitance and the series LC filter of the ATF, series LC resonance or "short circuit" can be generated at the resonance frequency of the QSG. In order to bypass the switching harmonics of the main VSI, the QSG should be placed at each of the sideband harmonics of the switching frequency. The overall control system of the ATF is shown in Figure 4-3, where a dc-link control loop and the QSG bank can be observed. The frequency characteristic of the output impedance is shown in Figure 4-4 where QSGs are placed at 2 kHz and 3 kHz. It can be seen from the figure that the output impedance approaches zero at the targeted frequencies.

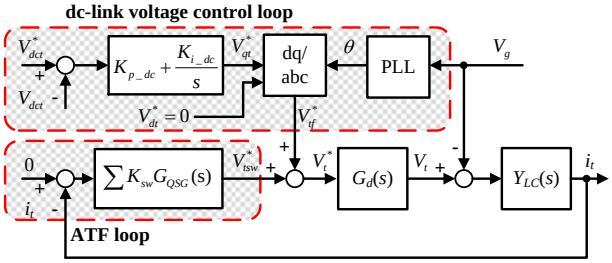

Figure 4-3. Overall control structure of the active trap filter, quoted from [120]

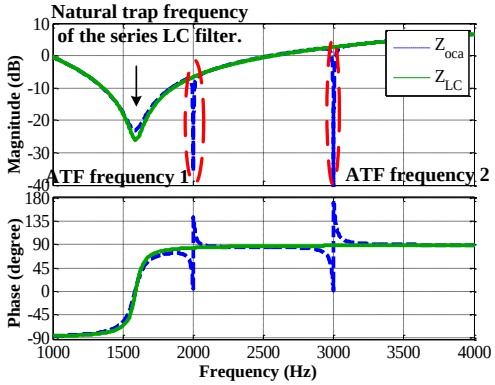

Figure 4-4. Frequency characteristic of the output impedance of ATF when QSGs are used at 2 kHz and 3 kHz, quoted from [120].

The performance of the active trap filter is tested experimentally and compared with the passive trap filters. The waveform of the grid current without enabling the ATF is shown in Figure 4-5(a), when the ATF is enabled, the grid current is shown in Figure 4-5(b). Quote from [120]: "The amplitude of the switching harmonics up to around 8 kHz were reduced by nearly 4 times". It should be noted that the sampling frequency of the ATF is 20 kHz, whose Nyquist frequency is 10 kHz. Using the conventional current control technique to control current at this high frequency is challenging since the current control bandwidth is usually 1/10 of the sampling frequency (in this case 1 kHz). The grid current with the passive trap filters tuned around the first sideband are shown in Figure 4-5(c) and (d), respectively. It can be seen that the passive trap filter attenuate one frequency component and higher order sideband harmonics are not attenuated. Also, there are some harmonic resonances around 1 kHz, which need passive damping resistance or active damping functions in the main VSI. The results show that the ATF has advantages over the passive trap filters such as more sidebands harmonics attenuated and less harmonic resonances.

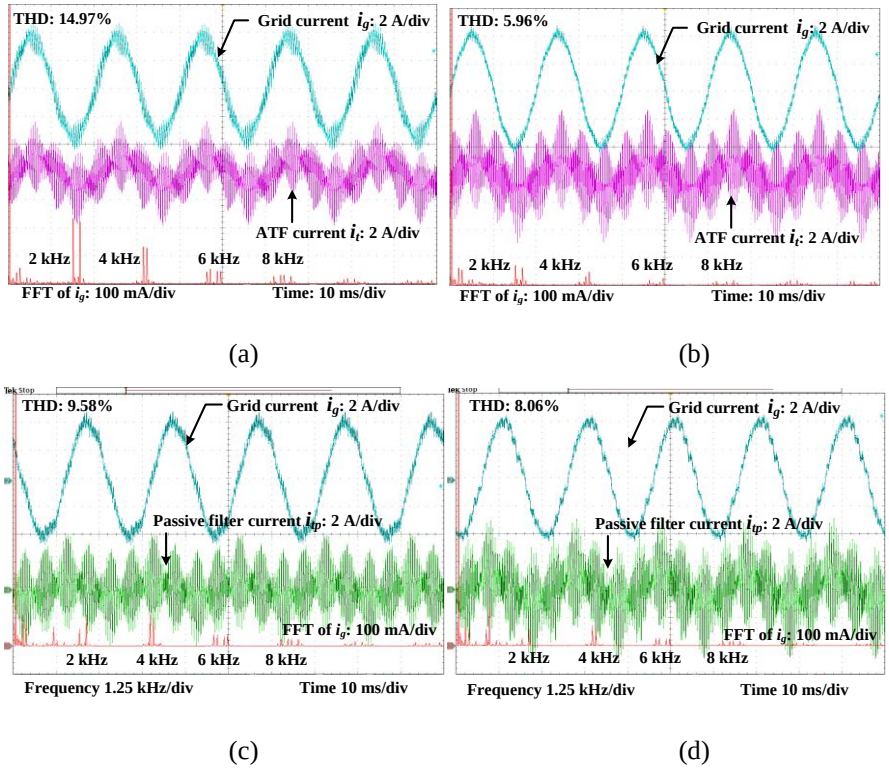

Figure 4-5. Performance of the proposed active trap filter and the passive trap filters, quoted from [120]. (a) grid current with passive trap filter tuned at 1.3 kHz, (b) grid current enabling the active trap filter, (c) grid current with passive trap filter tuned at 1.85 kHz, (d) grid current with passive trap filet tuned at 2.05 kHz.

4.2. KEY CONTRIBUTIONS

The impedance modelling method has been intensively adopted in the stability analysis of grid connected converters. The main contribution of this chapter is the physical interpretation of the current controllers in the impedance model and using the virtual impedance introduced by the current controller for harmonic attenuation. The current controller show resistive and capacitive response to voltage disturbance. The response is independent of the current reference and the current reference can be set to zero. In this chapter, virtual capacitance is introduced with QSG at the sideband harmonics of the main VSI. Compared with the passive filtering techniques, the proposed method has the advantages of reduced passive trap branches and improved system stability. Compared with the conventional active power filtering techniques, the advantages of the proposed method are the reduced complexity of the controller and higher frequency range for harmonics compensation.

This chapter contributes to achieve research objective 2) in *Chapter 1.5*. With the proposed method the series LC filtered VSI can be integrated into the high power VSI for switching harmonic attenuation.

CHAPTER 5.

Paper 4

Harmonic Analysis and Mitigation of Low-Frequency Switching Voltage Source Inverter with Series LC Filtered VSI

Haofeng Bai, Xiongfei Wang, Poh Chiang Loh, Frede Blaabjerg

The paper has been submitted to
IEEE Journal of Emerging and Selected Topics on Power Electronics.

5.1. BRIEF SUMMARY

Due to the low switching frequency, the current control bandwidth of the high power Voltage Source Inverter (VSIs) is limited. The output current of the high power VSI can be distorted by the background harmonics in the grid voltage [45]. In this paper, a new control system is proposed for the Active Trap Filter so that it guarantees the sinusoidal output current of the main VSI even in the presence of grid harmonics. The topology of the studied system is shown in Figure 5-1. The system is composed of a high power VSI with low switching frequency and a series LC filtered Active Trap Filter (ATF). In order to derive the operation principles of the ATF, the impedance models of the system should be built. Since the low order harmonics in

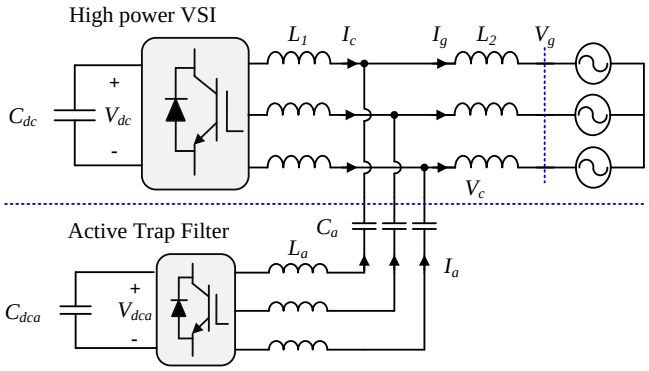

Figure 5-1. System topology of high power VSI with series LC filtered active trap filter, quoted from [121].

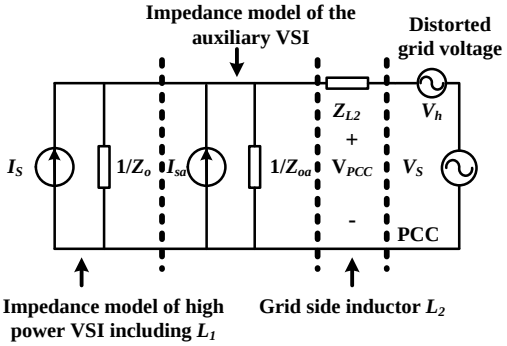

Figure 5-2. Impedance model of the system in Figure 5-1 at the background harmonic frequencies, quoted from [121].

the grid voltage are below the Nyquist frequency of the high power VSI, the Norton equivalent circuits are developed for both the high power VSI and the ATF. The impedance model of the system is shown in Figure 5-2. It should be noted that the model is not valid at the switching harmonics of the high power VSI.

Based on Figure 5-2, the harmonic component in the grid current can be obtained as

$$I_{g\_h} = \frac{I_{sa} Z_o Z_{oa}}{Z_o Z_{oa} + Z_o Z_{L2} + Z_{oa} Z_{L2}} - \frac{V_h \left(Z_o + Z_{oa} \right)}{Z_o Z_{oa} + Z_o Z_{L2} + Z_{oa} Z_{L2}} \tag{5.1}$$

In order to make I_{g_h} equal to zero, the following equation should hold.

$$I_{sa} = V_h \left(\frac{1}{Z_o} + \frac{1}{Z_{oa}} \right) \tag{5.2}$$

The above equation indicates that when the grid current is sinusoidal, the harmonic grid voltage is applied to only the output impedance of both the high power VSI and the ATF. Hence, the harmonic voltage can be virtually moved from the PCC point to the middle point between the two filter inductors. At the inverter side of the high power VSI, the harmonic current can be calculated as

$$I_{c\_h} = -\frac{V_h}{Z_o} \tag{5.3}$$

If the output impedance of the ATF Z_{oa} at the low order harmonics can be viewed as infinite (open circuit), then the harmonic current flowing into the ATF can be calculated as

$$I_{sa} = \frac{V_h}{Z_o} = -I_{c\_a} \tag{5.4}$$

The equation shows that the ATF should generate the current with the opposite phase with the harmonics at the inverter side of the high power VSI. At the switching harmonics, the ATF should provide zero output impedance to bypass the switching ripple. At the fundamental frequency, the ATF should regulate the dc-link voltage. The resultant overall control structure of the ATF is shown in Figure 5-3. In the figure, there are three control loops, namely the ATF loop, the APF loop and the dc-link control loop. The three control loops should work in different frequency ranges in order not to interfere with each other. The closed-loop gain of the dc-link control loop can be calculated as

$$G_{cl\_dc} = \frac{2\xi\omega_{dc} s + \omega_{dc}^2}{s^2 + 2\xi\omega_{dc} s + \omega_{dc}^2} \tag{5.5}$$

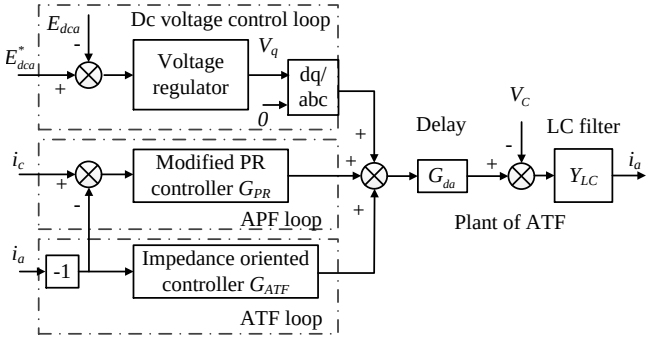

Figure 5-3. Overall control structure of the ATF, quoted from [121].

where

$$\omega_{dc} = \sqrt{K_{i\_dc} I_{g0}}, \quad \xi = 2K_{p\_dc}\sqrt{\frac{I_{g0}}{K_{i\_dc}}} \tag{5.6}$$

are the natural frequency and damping ratio of the dc-link control loop, respectively. By setting the damping ratio ξ to the typical value of 0.707 and the bandwidth ω_{b_dc} below the fundamental frequency, the control gains can be obtained as

$$K_{p\_dc} = \frac{0.47\omega_{b\_dc}}{I_{g0}} \tag{5.7}$$

$$K_{\mathrm{i}\_dc} = \frac{0.23\omega_{b\_dc}^2}{I_{g0}} \tag{5.8}$$

Experiments are carried out to test the performance of the proposed control strategy. A programmable AC source is used as the grid voltage and the 13th harmonic is injected into the grid voltage. The grid voltage, grid current, inverter current of the high power VSI is shown in Figure 5-4 when the ATF loop is disconnected. As it can be seen, the grid current I_g contain both switching harmonics and the 13th harmonics. When the ATF is connected without enabling the APF loop, the experimental results are shown in Figure 5-5, where the grid current I_g is distorted with 13th harmonic and the ATF current I_a is heavily distorted with the switching harmonics. When both the APF loop and ATF loop are enabled, the experimental results are shown in Figure 5-6, where the grid current I_g is sinusoidal. The performance of the dc-link control loop is shown in Figure 5-7, where the dc-link voltage is stepped from 400 V to 200 V. The dynamic process takes about 0.8 s.

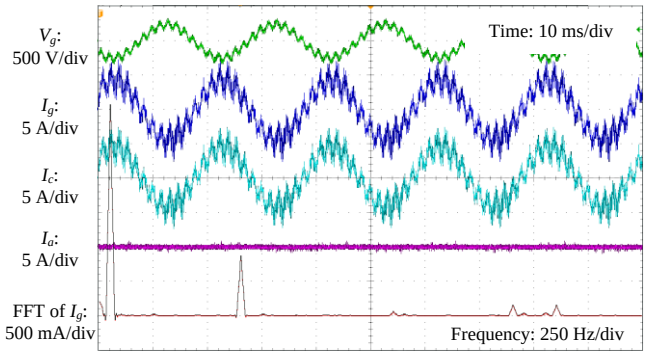

Figure 5-4. Experimental results when ATF is disconnected, quoted from [121].

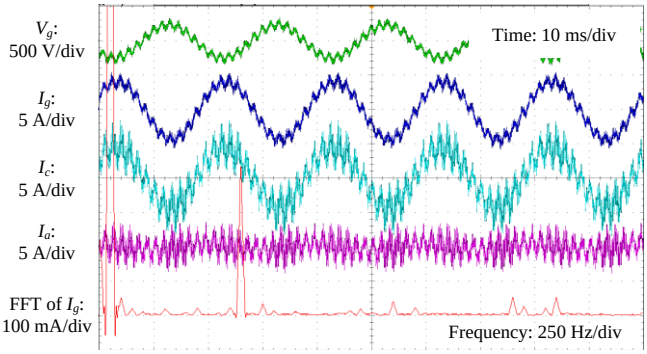

Figure 5-5. Experimental results when APF loop is disabled, quoted from [121].

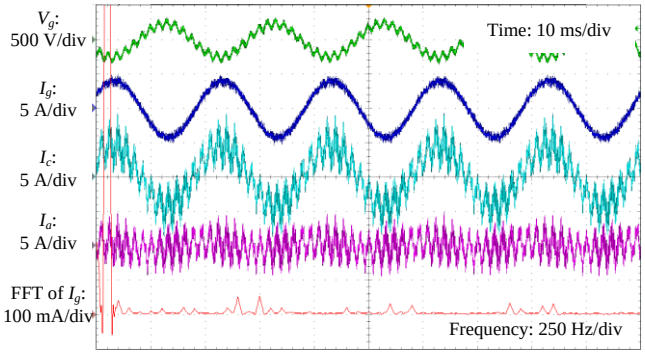

Figure 5-6. Experimental results when both APF loop and ATF loop are enabled, quoted from [121].

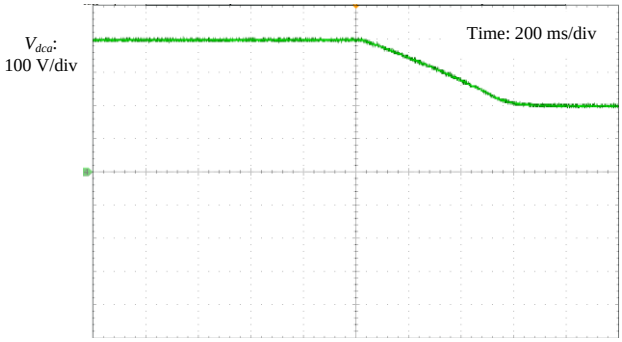

Figure 5-7. Performance of the dc-link control loop, quoted from [121].

5.2. KEY CONTRIBUTIONS

The main contribution of this chapter is the systematic method to integrate the series LC filtered ATF with the high power VSIs. The impedance model of the system is first derived to get the operation target for the ATF. In order to guarantee a sinusoidal grid current, the output impedance of the ATF should be high at the low order harmonics. Then three control loops are developed for different frequency ranges. The ATF loop works at the sideband frequencies, the APF loop works at the low order harmonics and the dc-link control loop works below the fundamental frequency. Finally, the performance of the developed control system is verified experimentally.

This chapter contributes to achieve research objective 2) in the introduction part. With the proposed method the series LC filtered VSI can be integrated into the high power VSI for low order harmonic attenuation.

CHAPTER 6.

Paper 5

A Grid-Voltage-Sensorless Resistive Active Power Filter with Series LC-Filter

Haofeng Bai, Xiongfei Wang, Frede Blaabjerg

The paper has been accepted by
IEEE Transactions on Power Electronics
10.1109/TPEL.2017.2717183

6.1. BRIEF SUMMARY

The Resistive-Active Power Filter (R-APF) has been widely used to dampen the low order harmonic resonances in the power grid and isolate the propagation of harmonic voltages [79]-[83]. Even though voltage sensorless control has been developed for normal voltage source inverter [107], the voltage sensorless control of the R-APF has been rarely reported. In this paper a single phase AC voltage sensorless R-APF is proposed. Without the AC voltage sensor, the isolation between the power stage and the control circuit of the converter can be improved, which may lead to increased system reliability. Also the system cost will be reduced. The topology of the series LC filtered R-APF is shown in Figure 6-1.

For the conventional control of R-APF, the grid voltage needs to be measured for two purposes: 1) current reference generation and 2) grid synchronization [65]. The current reference is often calculated by dividing the harmonic voltage with the damping resistance. The grid synchronization is necessary for the dc-link voltage control. A typical control structure of the R-APF is shown in Figure 6-2.

The proposed control structure of the series LC filtered R-APF is shown in Figure 6-3. Instead of tracking certain current reference, the output impedance of the series LC filtered R-APF is utilized to provide the desired virtual resistance. Moreover, a

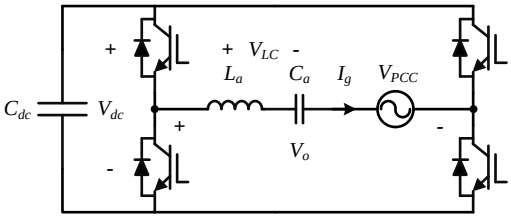

Figure 6-1. Topology of the single phase LC filtered R-APF, quoted from [122].

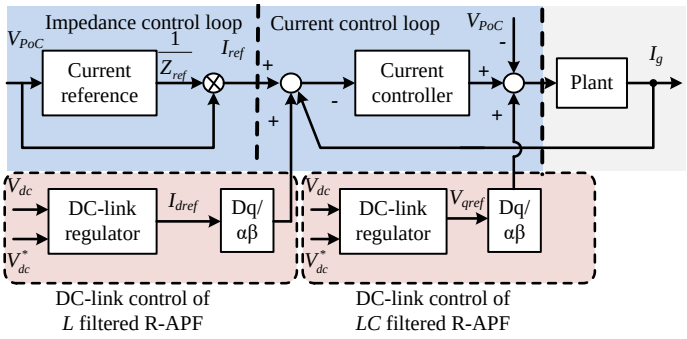

Figure 6-2. Typical control structure of the R-APF, quoted from [122].

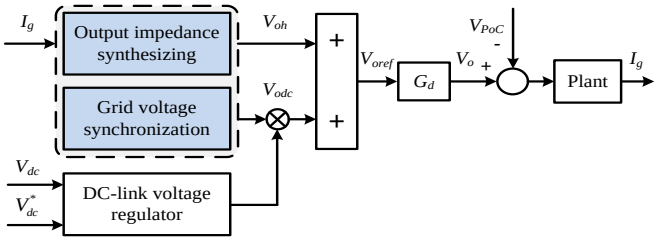

Figure 6-3. Structure of proposed AC voltage sensorless R-APF, quoted from [122].

fundamental grid voltage estimation method is proposed, so that only the output current of the R-APF needs to be measured.

The output impedance synthesizing block is shown in Figure 6-4. It is composed of a virtual capacitance generation block, a virtual resistance generation block and a deadtime compensation block. The virtual capacitance is introduced by paralleled Quadrature Signal Generators (QSGs). In order to isolate the nearby harmonics, a comb-based pre-filter is adopted. Compared with the paralleled Second Order Generalized Integrator (SOGI) technique, the comb-filter is simple and is easy to tune [116]. The virtual resistance is introduced by a proportional controller with the damping resistance as the gain. In real applications, deadtime is inserted before the turn-on instant of the semiconductor devices in order to avoid short circuit. This deadtime will introduce low order distortion in the output voltage [40] and affect the virtual resistance emulation of the R-APF. In this paper, a square wave is injected into the voltage reference to compensate the deadtime effect. The structure of the deadtime compensation block is shown in Figure 6-5.

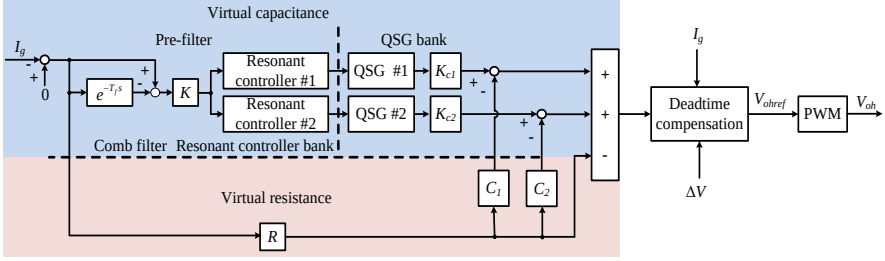

Figure 6-4. Structure of the output impedance synthesizing block, quoted from [122].

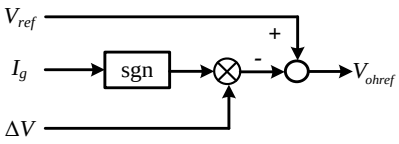

Figure 6-5. Deadtime compensation block, quoted from [122].

At the fundamental frequency, the output current of the R-APF is determined by the difference between the grid voltage and its output voltage. With the output current I_g and the output voltage V_o, the grid voltage can be estimated using the following KVL equation.

$$V_{PoC}(j\omega) = \underbrace{V_o(j\omega)}_{\text{output voltage}} - \underbrace{Z_{LC}(j\omega) I_g(j\omega)}_{\text{voltage accross the LC filter}} \quad (6.1)$$

$$\text{where} \qquad Z_{LC}(j\omega) = \frac{1}{j\omega C_a} - j\omega L_a$$

The resultant dc-link voltage control block is shown in Figure 6-6. In the figure, the output current I_g is fed to a QSG tuned at the fundamental frequency. The output of the QSG is then multiplied with the impedance of the LC filter at the fundamental frequency, which is the voltage dropped on the series LC filter. The grid voltage is the sum of V_{oref} and V_{LCe} neglecting the distortion introduced by the Pulse Width Modulation (PWM) process. The output of the dc-link voltage regulator is then aligned to the quadrature signal of the estimated grid voltage. It should be noted that if the dc-link voltage of the R-APF is low, the output current I_g is naturally aligned to the quadrature of the grid voltage.

In order to test the performance of the proposed sensorless control of the R-APF, experiments are carried out. A programmable AC source is used to provide the harmonics in the grid voltage at 5th and 7th harmonic. The waveforms of the grid voltage and the output current are shown in Figure 6-7 where the resistance of the R-APF is set to 10 Ω. The harmonic components are then extracted in the Matlab environment using the *fft* and *ifft* function. The waveforms of the extracted harmonic voltage and current are shown in Figure 6-8. From the figure the desired the impedance can be observed. The same procedure has been done with the resistance set to 20 Ω. The impedance characteristic is summarized in Table 6.1. From the table it can be seen that the R-APF emulates the resistance with good accuracy.

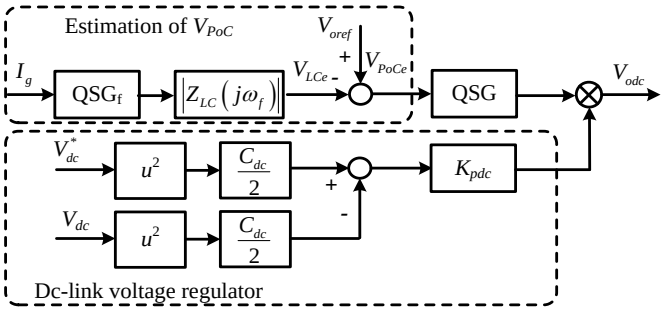

Figure 6-6. Dc-link voltage control loop of the sensorless R-APF, quoted from [122].

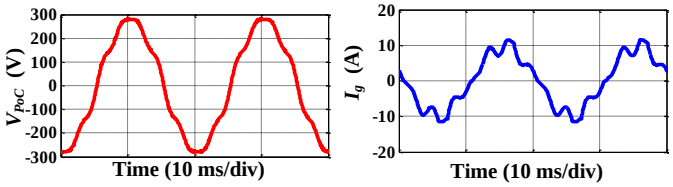

(a) (b)

Figure 6-7. Waveforms of the distorted grid voltage and the output current of the R-APF, quoted from [122]. (a) grid voltage, (b) output current of the R-APF.

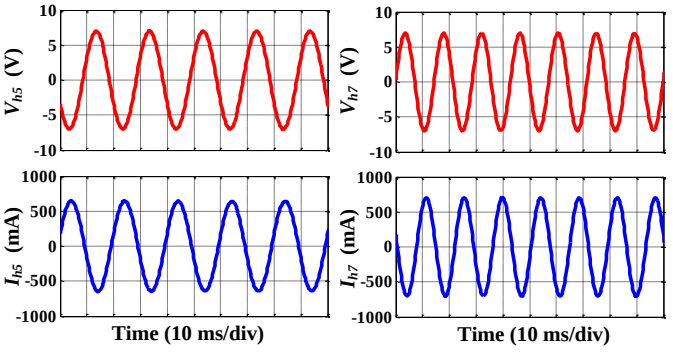

(a) (b)

Figure 6-8. Extracted harmonic voltage and current, quoted from [122]. (a) 5^{th} harmonic voltage and current, (b) 7^{th} harmonic voltage and current.

Table 6.1. Measured impedance characteristic of the R-APF, quoted from [122]

R \ h	5^{th}	7^{th}
$10\ \Omega$	$10.7\angle 13.5^{\circ}$	$10.2\angle 18.9^{\circ}$
$20\ \Omega$	$20.6\angle 4.5^{\circ}$	$18.5\angle 0^{\circ}$

The performance of the dc-link control loop is shown in Figure 6-9, where the dc-link voltage is changed from 300 V to 200 V. The waveform of V_{dc} is shown in Figure 6-9(a). In the steady state the tracking error is below 2 V. The dynamic process takes about 4 fundamental cycles. The real and estimated grid voltage are shown in Figure 6-9(b). In the steady state, there is little estimation error and during the transient process, there is small estimation error.

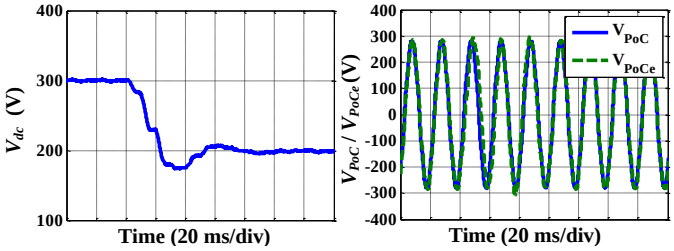

(a) (b)

Figure 6-9. Performance of the dc-link voltage control loop, quoted from [122]. (a) waveform of V_{dc} and (b) estimation of the grid voltage.

6.2. KEY CONTRIBUTIONS

The key contribution of this chapter is the estimation method of the fundamental grid voltage for the series LC filtered R-APF. With the proposed fundamental voltage estimation method, the output of the dc-link regulator can be synchronized with the grid, enabling the AC voltage sensorless control of the R-APF. Moreover, incremental contributions are made to allow the R-APF to mimic damping resistance at multiple frequencies with a comb-based pre-filter. The deadtime effect is also compensated using a simple open-loop method.

This chapter achieves research objective 3) in the introduction part. With the proposed method, the series LC filtered VSI can be used to dampen the LCC originated harmonics resonance in the PE based power system.

CHAPTER 7. CONCLUSIONS

7.1. THESIS SUMMARY

In this thesis, the three harmonic issues in the modern PE based power system are addressed using the impedance model of series LC filtered VSI. The series LC filtered VSI has been useful in the stabilisation of the PE based power sytem and low order harmonic resonance damping. The hypothesizes listed in Chapter 1.4 are verified and the research objectives listed in Chapter 1.5 are achieved using the output impedance of the series LC filtered VSI.

To be more specific, the following researches have been done.

1) Harmonic Stabilization with Improved Control of Series LC Filtered Active Damper

The stability analysis regarding the passivity of the PE based power plant has been carried out in Chapter 2 and Chapter 3. In a PE based power system with multiple grid-connected VSIs, each VSI can be represented in the Norton equivalent circuit. The real-part of the output admittance is investigated in order to identify the non-passive frequency region. It is shown that the system stability can be improved by enhancing the passivity of the system. The operation principle of the active damper is changed to enhance the passivity of the system, which allows a simple proportional current controller to be used. The online detection of the resonance frequency hence becomes unnecessary for the active damper.

From the impedance point of view, an active damper is not the only choice for the passvity enhancement. As long as the real part of the output admittance is positive, the grid-connected VSI can be viewed as a generalized active damper. In this thesis, it is proved that the paralleled LCL filtered VSIs with different system parameters and control strategies can provide the damping function for each other. Three cases are studied where no active damping is applied to the VSIs. The system stability is improved with the combination of different VSIs. The non-passive region has been calculated analytically with simple expressions which can be used easily by engineers. Nevertheless, the numerical calculations can also be used to find the potential combinations of VSIs. Also the VSIs with an active damping funtion can be investigated in respect to the non-passivity region.

2) Integration of Series LC Filtered VSI with High Power VSI

The control system of the series LC filtered VSI has been developed in Chapter 4 and Chapter 5, so that it can attenuate both the switching harmonics of the high power VSI and the low order harmonics introduced by the grid voltage distortion. In

the developed control system, special current controllers are designed based on the Quadrature Signal Generator (QSG) to provide zero output impedance at the sideband frequencies of the high power VSI. The developed series LC filtered VSI is denoted as "Active Trap Filter (ATF)". Like the passive trap filters, the ATF bypasses the switching harmonics with a low impedance path.

The impedance model of a high power VSI with an ATF is developed in different frequency ranges. The impact of the distorted grid voltage and the corresponding harmonic current distributions are analyzed based on the impedance model. The control targets and implementation are developed so that the ATF can guarantee a sinusoidal output current with low switching ripple even in the presence of background harmonics.

3) AC Voltage Sensorless Control of Series LC Filtered R-APF

Based on the output impedance shaping method of the series LC filtered VSI proposed in Chapter 4, the proposed R-APF emulates the virtual resistance without measuring the grid voltage in Chapter 6. In order to completely remove the AC voltage sensors, a fundamental grid voltage estimation method is proposed. With the proposed grid estimation method, the output of the dc-link regulator is aligned to the q-axis. Both the dc-link control and the resistance emulation can be achieved without any AC voltage sensor.

7.2. RESEARCH CONTRIBUTIONS

In this thesis, the three research objectives in *Chapter 1.5* are achieved with proposed control strategies of the series LC filtered VSI from *Chapter 2* to *Chapter 6*. In *Chapter 2* and *3*, the series LC filtered VSI is used to stabilize the PE based power system, achieving research objective 1). In *Chapter 4* and *5*, new control method is proposed to integrate the series LC filtered VSI into the high power VSI for harmonic attenuation both at switching frequencies and low order harmonics, achieving research objective 2). In *Chapter 6*, new control strategy is proposed for the series LC filtered VSI to dampen the low order harmonic resonance in the PE based power system, achieving research objective 3). To be more specific, this work has the following contributions to the state of art:

- Impedance based model of grid-connected VSIs is applied to the analysis of stability and passivity of the output admittance is investigated in *Chapter 2* and *3*. A deeper understanding of the mechanism of the active damper is obtained. The operation principle of the active damper is changed from mimicking resistive behavior to the enhancement of passivity in *Chapter 3*. The benefits from this work include:

- The frequency detection of the harmonic resonance becomes no longer necessary for the active damper;
- Normal LCL filtered VSIs with different parameters can provide the function of active damper to the PE based power system.

- In this thesis, the output impedance of a current controlled VSI is first utilized for source-originated harmonic attenuation, such as the switching harmonics of a high power VSI or the harmonics in the grid voltage. Instead of minimizing the output admittance, the output admittance is designed to provide the desired impedance characteristics. By utilizing the output impedance, an accurate current tracking can be avoided, which overcome some challenges with this system. For example, the ATF can attenuate switching harmonics of a high power VSI up to 8 kHz with a sampling frequency of 20 kHz in *Chapter 4*. Tuning of the current controller using the traditional method would require complex calculation and has only been applied successfully on L filtered VSIs. What is more, the current reference can be set to zero, which reduces the requirement for load current / voltage measurement.

- The possibility of using an impedance model for harmonic mitigation in a PE based power system has been verified. Three specific applications have been proved potentially viable at least in the lab.

  - For the low order harmonics, the AC voltage sensorless R-APF has been proposed in *Chapter 6*. Compared with the traditional R-APF, the proposed R-APF control does not need the AC voltage sensor, which brings some potential advantages such as improved reliability and reduced cost.
  - For the harmonic resonance damping, the series LC filtered active damper is improved with a simple P controller in *Chapter 3*. Compared with the existing control method of the active damper, the operation principle is changed from mimicking a resistor to enhancing the passivity. Thus the harmonic resonance frequency detection is not needed.
  - For the active harmonic attenuation of a high power VSI, the ATF is proposed in *Chapter 4* and *5*. The switching harmonics are mitigated by introducing low impedance path with impedance-oriented current controller. The proposed control method is easy to tune and implement. Also, the ATF is able to compensate the low order harmonics introduced by the grid distortion.

7.3. FUTURE RESEARCH POSSIBILITIES

Based on the research in this work, the following aspects can be investigated in the future

- Practical real-life applications of the series LC filtered VSI studied in this thesis.
- The key component of the output impedance shaping method is the paralleled Quadrature Signal Generators (QSGs). Now the bandwidth of the QSG is tuned to achieve the tradeoff between the frequency selectivity and the robustness to frequency variation. The structure of the paralleled QSG can be improved to avoid this tradeoff.
- The bandwidth of the control loops of the series LC filtered VSI are separated in the frequency domain. The dc-link control loop has low control bandwidth in order not to interfere with other control loop. The decoupling between the dc-link control loop and other control loops should be studied in order to improve the performance of the series LC filtered VSI.
- The proposed output impedance shaping method can be applied to the control of the series LC filtered VSI in other applications, such as the inductive power transfer, where a similar topology is used and the resonance frequency is high.
- Since the series LC filtered VSI requires very low dc-link voltage, low voltage devices such as Cool-Mos and GaN can be used to increase the switching frequency. The control performance of the proposed ATF and R-APF can thus be improved. The multilevel topology can also be studied for medium voltage distribution network.
- The protection of the series LC filtered VSI during transients and grid fault conditions.
- The resonance frequency detection of the PE based power system.

BIBLIOGRAPHY

[1] F. Blaabjerg, Zhe Chen and S. B. Kjaer, "Power electronics as efficient interface in dispersed power generation systems," *IEEE Trans. Power Electron.*, vol. 19, no. 5, pp. 1184-1194, Sept. 2004.

[2] J. Arai, K. Iba, T. Funabashi, Y. Nakanishi, K. Koyanagi and R. Yokoyama, "Power electronics and its applications to renewable energy in Japan," *IEEE Circuits Syst. Mag*, vol. 8, no. 3, pp. 52-66, Third Quarter 2008.

[3] J. Rocabert, A. Luna, F. Blaabjerg and P. Rodríguez, "Control of power converters in AC microgrids," *IEEE Trans. Power Electron.*, vol. 27, no. 11, pp. 4734-4749, Nov. 2012.

[4] G. Oriti, A. L. Julian and N. J. Peck, "Power-electronics-based energy management system with storage," *IEEE Trans. Power Electron.*, vol. 31, no. 1, pp. 452-460, Jan. 2016.

[5] X. Wang, F. Blaabjerg and W. Wu, "Modeling and analysis of harmonic stability in an AC power-electronics-based power system," *IEEE Trans. Power Electron.*, vol. 29, no. 12, pp. 6421-6432, Dec. 2014.

[6] IEEE Working Group on Power System Harmonics, "Power system harmonics: an overview," *IEEE Trans. Power Apparat. Syst.*, vol. PAS- 102, no. 8, pp. 2455-2459, Aug. 1983.

[7] J. C. Read, "The calculation of rectifier and inverter performance characteristics," in *Electrical Engineers - Part II: Power Engineering, Journal of the Institution of*, vol. 92, no. 29, pp. 495-509, October 1945.

[8] V. E. Wanger, "Effects of harmonics on equipment," *IEEE Trans. Power Del.*, vol. 8, no. 2, pp. 672–680, Apr. 1993.

[9] J. J. Mesas, L. Sainz and A. Ferrer, "Deterministic and stochastic study of the three-phase non-linear load behavior," in *Proc. of IEEE International Conference on Power Engineering, Energy and Electrical Drives, POWERENG '09, Lisbon, Portugal, March 18-20, 2009*, pp. 297-302.

[10] R. Arseneau, Y. Baghzouz, J. Belanger, K. Bowes, A. Braun, A. Chiaravllo, M. Cox, S. Crampton, A. Emauel, P. Filipski, E. Gunther, A. girgis, D. Hartmann, S. He, G. Hensley, D. Lwanusiw, W. Kortebein, T. McComb, A. McEachern, T. Nelson, N. Oldham, D. Piehl, K. Srinivasan, R. Stevens, T. Unruh, D. Williams, "A survey of North American electric utility concerns regarding nonsinusoidal waveforms," *IEEE Trans. Power Del.*, vol. 11, no. 1, pp. 73-78, Jan 1996.

[11] M. Sakui and H. Fujita, "An analytical method for calculating harmonic

currents of a three-phase diode-bridge rectifier with DC filter," *IEEE Trans. Power Electron.*, vol. 9, no. 6, pp. 631-637, Nov 1994.

[12] R. D. Henderson and P. J. Rose, "Harmonics: the effects on power quality and transformers," *IEEE Trans. Ind. Appl.*, vol. 30, no. 3, pp. 528-532, May/Jun 1994.

[13] J. S. Subjak and J. S. McQuilkin, "Harmonics-causes, effects, measurements, and analysis: an update," *IEEE Trans. Ind. Appl.*, vol. 26, no. 6, pp. 1034-1042, Nov/Dec 1990.

[14] A. Medina, J. Segundo-Ramirez, P. Ribeiro, W. Xu, K. L. Lian, G. W. Chang, V. Dinavahi, and N. R. Waston, "Harmonic analysis in frequency and time domain," *IEEE Trans. Power Del.*, vol. 28, no. 3, pp. 1813-1821, July 2013.

[15] H. Suryanarayana; S. D. Sudhoff, "Design paradigm for power electronics based DC distribution systems," *IEEE J. Emerg. Sel. Topics Power Electron.*, vol. 5, no. 1, pp. 51-63, March 2017.

[16] S. Grunau and F. W. Fuchs, “Effect of wind-energy power injection into weak grids,” in *Proc. of EWEA*, 2012, pp. 1–7.

[17] M. Liserre, R. Cardenas, M. Molinas and J. Rodriguez, "Overview of multi-MW wind turbines and wind Parks," *IEEE Trans. Ind. Electron.*, vol. 58, no. 4, pp. 1081-1095, April 2011.

[18] Y. Song; F. Blaabjerg, "Overview of DFIG-based wind power system resonances under weak networks," *IEEE Trans. Power Electron.* , vol. 32, no. 6, pp. 4370-4394, June 2017.

[19] F. Blaabjerg, Zhe Chen and R. Teodorescu, "Renewable energy systems in the power electronics curriculum," in *Proc. Of IEEE Workshop on Power Electronics Education*, pp. 58- 68, 2005.

[20] F. Blaabjerg, F. Iov, T. Kerekes and R. Teodorescu, "Trends in power electronics and control of renewable energy systems," in *Proc. 14th Int. EPE Power Electron. Motion Control Conf.*, Sep. 2010, pp. 1–19.

[21] F. Blaabjerg, R. Teodorescu, M. Liserre and A. V. Timbus, "Overview of control and grid synchronization for distributed power generation systems," *IEEE Trans. Ind. Electron.*, vol. 53, no. 5, pp. 1398-1409, Oct. 2006.

[22] L. Harnefors, X. Wang, A. G. Yepes and F. Blaabjerg, "Passivity-based stability assessment of grid-connected VSCs—an overview," *IEEE J. Emerg. Sel. Topics Power Electron.*, vol. 4, no. 1, pp. 116-125, March 2016.

[23] L. Harnefors, “Modelling of three-phase dynamic systems using complex transfer functions and transfer matrices,” I*EEE Trans. Ind. Electron.*, vol. 54, no. 4, pp. 2239–2248, Aug. 2007.

[24] B. Wen, D. Boroyevich, R. Burgos, P. Mattavelli, and Z. Shen, “Analysis of D-Q small-signal impedance of grid-tied inverters,” *IEEE Trans. Power Electron.*, vol. 31, no. 1, pp. 675–687, Jan. 2016.

[25] H. Yi, X. Wang, F. Blaabjerg and F. Zhuo, "Impedance Analysis of SOGI-FLL-Based Grid Synchronization," *IEEE Trans. Power Electron.*, vol. 32, no. 10, pp. 7409-7413, Oct. 2017.

[26] J. L. Agorreta, M. Borrega, J. López and L. Marroyo, "Modeling and control of N-paralleled grid-connected inverters with LCL filter coupled due to grid impedance in PV plants," *IEEE Trans. Power Electron.*, vol. 26, no. 3, pp. 770-785, March 2011.

[27] A. Emadi, K. Rajashekara, S. S. Williamson and S. M. Lukic, "Topological overview of hybrid electric and fuel cell vehicular power system architectures and configurations," *IEEE Trans. Veh. Technol.*, vol. 54, no. 3, pp. 763-770, May 2005.

[28] C. C. Chan, "The state of the art of electric, hybrid, and fuel cell vehicles," in *Proceedings of IEEE*, vol. 95, no. 4, pp. 704-718, April 2007.

[29] M. E. Raoufat; A. Khayatian; A. Mojallal, "Performance recovery of voltage source converters with application to grid-connected fuel cell DGs," *IEEE Trans. Smart Grid*, vol.PP, no.99, pp.1-8.

[30] A. Emadi, Y. J. Lee and K. Rajashekara, "Power electronics and motor drives in electric, hybrid electric, and plug-in hybrid electric vehicles," *IEEE Trans. Ind. Electron.*, vol. 55, no. 6, pp. 2237-2245, June 2008.

[31] H. Akagi and T. Shimizu, "Attenuation of conducted EMI emissions from an inverter-driven motor," *IEEE Trans. Power Electron.*, vol. 23, no. 1, pp. 282-290, Jan. 2008.

[32] V. V. Aban and A. M. Hava, "Performance analysis, filter component sizing, and controller structure selection of small capacitor diode rectifier front end inverter drives," in *Proc. 16th Int. EPE Power Electron. Motion Control Conf.*, 2014, pp. 745-750.

[33] X. Wang, F. Blaabjerg, M. Liserre, Z. Chen, J. He and Y. Li, "An active damper for stabilizing power-electronics-based AC systems," *IEEE Trans. Power Electron.*, vol. 29, no. 7, pp. 3318-3329, July 2014.

[34] E. Mollerstedt and B. Bernhardsson, "Out of control because of harmonics-an analysis of the harmonic response of an inverter locomotive," *IEEE Control Systems*, vol. 20, no. 4, pp. 70-81, Aug. 2000.

[35] J. H. R. Enslin and P. J. M. Heskes, "Harmonic interaction between a large number of distributed power inverters and the distribution network," *IEEE Trans. Power Electron.*, vol. 19, no. 6, pp. 1586-1593, Nov. 2004.

[36] Q. Ye, R. Mo, Y. Shi and H. Li, "A unified Impedance-based Stability Criterion (UIBSC) for paralleled grid-tied inverters using global minor loop gain (GMLG)," in *Proc. Conf. IEEE Energy Convers. Congr. Expo.*, 2015, pp. 5816-5821.

[37] M. Liserre, R. Teodorescu and F. Blaabjerg, "Stability of grid-connected PV inverters with large grid impedance variation," in *Proc. IEEE 35th Annu. Power Electron. Spec. Conf.*, Jun. 2004, vol. 6, pp. 4773–4779.

[38] J. Sun, "Impedance-based stability criterion for grid-connected inverters," *IEEE Trans. Power Electron.*, vol. 26, no. 11, pp. 3075-3078, Nov. 2011.

[39] Y. Sun, C. Dai, J. Li and J. Yong, "Frequency-domain harmonic matrix model for three-phase diode-bridge rectifier," *IET Gener. Trans. Distrib.*, vol. 10, no. 7, pp. 1605-1614, 2016.

[40] D. G. Holmes and T. A. Lipo, *Pulse Width Modulation for Power Converters: Principles and Practice*. Hoboken, NJ: IEEE Press and Wiley Interscience, 2003.

[41] R.W. Erickson and D. Maksimovic, *Fundamentals of Power Electronics*, 2nd ed. Norwell, MA, USA: Kluwer, 2001

[42] R. N. Beres, X. Wang, F. Blaabjerg, M. Liserre and C. L. Bak, "Optimal design of high-order passive-damped filters for grid-connected applications," *IEEE Trans. Power Electron.*, vol. 31, no. 3, pp. 2083-2098, March 2016.

[43] M. A. Elsaharty, "Passive L and LCL filter design method for grid-connected inverters," in *Proc. IEEE ISGT*, 2014, pp. 31–34.

[44] M. Liserre, F. Blaabjerg and S. Hansen, "Design and control of an LCL-filter-based three-phase active rectifier," *IEEE Trans. Ind. Appl.*, vol. 41, no. 5, pp. 1281-1291, Sept.-Oct. 2005.

[45] A. A. Rockhill, M. Liserre, R. Teodorescu and P. Rodriguez, "Grid-filter design for a multimegawatt medium-voltage voltage-source inverter," *IEEE Trans. Ind. Electron.*, vol. 58, no. 4, pp. 1205-1217, April 2011.

[46] X. Li, X. Wu, Y. Geng, X. Yuan, C. Xia and X. Zhang, "Wide damping region for LCL-type grid-connected inverter with an improved capacitor-current-feedback method," *IEEE Trans. Power Electron.*, vol. 30, no. 9, pp. 5247-5259, Sept. 2015.

[47] Y. Tang, P. C. Loh, P. Wang, F. H. Choo, F. Gao and F. Blaabjerg, "Generalized design of high performance shunt active power filter with output LCL filter," *IEEE Trans. Ind. Electron.*, vol. 59, no. 3, pp. 1443-1452, March 2012.

[48] W. Wu, Y. He and F. Blaabjerg, "An LLCL power filter for single-phase

grid-tied inverter," *IEEE Trans. Power Electron.*, vol. 27, no. 2, pp. 782-789, Feb. 2012.

[49] W. Wu, Y. He, T. Tang and F. Blaabjerg, "A new design method for the passive damped LCL and LLCL filter-based single-phase grid-tied inverter," *IEEE Trans. Ind. Electron.*, vol. 60, no. 10, pp. 4339-4350, Oct. 2013.

[50] X. Zhang, H. Zhu, F. Li, F. Liu, C. Liu and B. Li, "An LCL-LC power filter for grid-tied inverter," in *Proc. 2013 IEEETENCON 2013*, Xi'an, 2013, pp. 1-4.

[51] M. Huang, X. Wang, P. C. Loh and F. Blaabjerg, "LLCL-filtered grid converter with improved stability and robustness," *IEEE Trans. Power Electron.*, vol. 31, no. 5, pp. 3958-3967, May 2016.

[52] S. Jiang, S. Zhang, X. Lu, B. Ge and F. Z. Peng, "Resonance issues and active damping in HVAC grid-connected offshore wind farm," in *Proc. IEEE ECCE*, Denver, CO, 2013, pp. 210-215.

[53] J. Sun, "Small-signal methods for AC distributed power systems–a review," *IEEE Trans. Power Electron.*, vol. 24, no. 11, pp. 2545-2554, Nov. 2009.

[54] M. Amin; M. Molinas, "Understanding the origin of oscillatory phenomena observed between wind farms and HVDC systems," *IEEE J. Emerg. Sel. Topics Power Electron.* , vol. 5, no. 1, pp. 378-392, March 2017.

[55] X. Wang, F. Blaabjerg and P. C. Loh, "Grid-current-feedback active damping for LCL resonance in grid-connected voltage-source converters," *IEEE Trans. Power Electron.*, vol. 31, no. 1, pp. 213-223, Jan. 2016.

[56] M. Liserre, R. Teodorescu and F. Blaabjerg, "Stability of photovoltaic and wind turbine grid-connected inverters for a large set of grid impedance values," *IEEE Trans. Power Electron.*, vol. 21, no. 1, pp. 263-272, Jan. 2006.

[57] L. Harnefors, L. Zhang and M. Bongiorno, "Frequency-domain passivity-based current controller design," *IET Power Electronics*, vol. 1, no. 4, pp. 455-465, Dec. 2008.

[58] I. Pendharkar, "A generalized input admittance criterion for resonance stability in electrical railway networks," in *Proc. ECC.*, 2014, pp. 690-695.

[59] L. Harnefors, M. Bongiorno and S. Lundberg, "Input-admittance calculation and shaping for controlled voltage-source converters," *IEEE Trans. Ind. Electron.*, vol. 54, no. 6, pp. 3323-3334, Dec. 2007.

[60] D. A. Gonzalez and J. C. McCall, "Design of filters to reduce harmonic distortion in industrial power Systems," *IEEE Trans. Ind. Appl.*, vol. IA-23, no. 3, pp. 504-511, May 1987.

[61] H. Akagi, "Trends in active power line conditioners," *IEEE Trans. Power*

Electron., vol. 9, no. 3, pp. 263-268, May 1994.

[62] Y. Sato, K. Kawamura, H. Morimoto and K. Nezu, "Hybrid PWM rectifiers to reduce electromagnetic interference," in *Proc. IEEE Ind. Appl. Soc. Annu. Meeting (IAS'02)*, 2002, pp. 2141–2146.

[63] S. Papadopoulos, M. Rashed, C. Klumpner and P. Wheeler, "Investigations in the modeling and control of a medium-voltage hybrid inverter system that uses a low-voltage/low-power rated auxiliary current source inverter," *IEEE J. Emerg. Sel. Topics Power Electron.*, vol. 4, no. 1, pp. 126-140, March 2016.

[64] S. Papadopoulos, M. Rashed, C. Klumpner and P. Wheeler, "A hybrid converter for medium voltage using a low-voltage current source active filter connected via a series capacitor," in P*roc. 16th Eur. Conf. Power Electron. Appl. (EPE-ECCE Europe)*, Aug. 2014, pp. 1–10.

[65] H. Akagi, "Modern active filters and traditional passive filters", *Bulletin of the polish academy of sciences*, vol. 54, no. 3, pp. 255-269, 2006.

[66] H. Fujita and H. Akagi, "A practical approach to harmonic compensation in power systems-series connection of passive and active filters," *IEEE Trans. Ind. Appl.*, vol. 27, no. 6, pp. 1020-1025, Nov/Dec 1991.

[67] H. Akagi, "New trends in active filters for power conditioning," *IEEE Trans. Ind. Appl.*, vol. 32, no. 6, pp. 1312-1322,

[68] S. A. Azmi, K. H. Ahmed, S. J. Finney and B. W. Williams, "Comparative analysis between voltage and current source inverters in grid-connected application," *IET Conference on Renewable Power Generation (RPG 2011)*, Edinburgh, 2011, pp. 1-6.

[69] B. Singh, K. Al-Haddad and A. Chandra, "A review of active filters for power quality improvement," *IEEE Trans. Ind. Electron.*, vol. 46, no. 5, pp. 960-971, Oct 1999.

[70] H. Fujita and H. Akagi, "The unified power quality conditioner: the integration of series and shunt-active filters," *IEEE Trans. Power Electron.*, vol. 13, no. 2, pp. 315-322, Mar 1998.

[71] F. Peng, "Application issues of active power filters," *IEEE Ind. Appl. Mag.*, vol. 4, no. 5, pp. 21-30, Sep/Oct 1998.

[72] F. Z. Peng, H. Akagi and A. Nabae, "A new approach to harmonic compensation in power systems-a combined system of shunt passive and series active filters," *IEEE Trans. Ind. Appl.*, vol. 26, no. 6, pp. 983-990, Nov/Dec 1990.

[73] P. Salmeron and S. P. Litran, "Improvement of the electric power quality using series active and shunt passive filters," *IEEE Trans. Power Del.*, vol.

25, no. 2, pp. 1058-1067, April 2010.

[74] X. Sun, R. Han, L. Yang, H. Shen,. Y. Tian, X. Guo, Z. Chen, "Study of a novel equivalent model and a long-feeder simulator-based active power filter in a closed-loop distribution feeder," *IEEE Trans. Ind. Electron.*, vol. 63, no. 5, pp. 2702-2712, May 2016.

[75] H. Akagi, H. Fujita and K. Wada, "A shunt active filter based on voltage detection for harmonic termination of a radial power distribution line," *IEEE Trans. Ind. Appl.*, vol. 35, no. 3, pp. 638-645, May/Jun 1999.

[76] H. Akagi, "Control strategy and site selection of a shunt active filter for damping of harmonic propagation in power distribution systems," *IEEE Trans. Power Del.*, vol. 12, no. 1, pp. 354-363, Jan 1997.

[77] H. Yi *et al*., "A source-current-detected shunt active power filter control scheme based on vector resonant controller," *IEEE Trans. Ind. Appl.*, vol. 50, no. 3, pp. 1953-1965, May-June 2014.

[78] L. Asiminoael, F. Blaabjerg and S. Hansen, "Detection is key - harmonic detection methods for active power filter applications," *IEEE Ind. Appl. Mag.*, vol. 13, no. 4, pp. 22-33, July-Aug. 2007.

[79] X. Sun, J. Zeng and Z. Chen, "Site selection strategy of single-frequency tuned R-APF for background harmonic Voltage damping in power systems," *IEEE Trans. Power Electron.*, vol. 28, no. 1, pp. 135-143, Jan. 2013.

[80] T. L. Lee, Y. C. Wang, J. C. Li and J. M. Guerrero, "Hybrid active filter with variable conductance for harmonic resonance suppression in industrial power systems," *IEEE Trans. Ind. Electron.*, vol. 62, no. 2, pp. 746-756, Feb. 2015.

[81] P. T. Cheng and T. L. Lee, "Distributed Active Filter Systems (DAFSs): A new approach to power system harmonics," *IEEE Trans. Ind. Appl.*, vol. 42, no. 5, pp. 1301-1309, Sept.-Oct. 2006.

[82] T. L. Lee and S. H. Hu, "Discrete frequency-tuning active filter to suppress harmonic resonances of closed-loop distribution power systems," *IEEE Trans. Power Electron.*, vol. 26, no. 1, pp. 137-148, Jan. 2011.

[83] R. B. Gonzatti, S. C. Ferreira, C. H. da Silva, R. R. Pereira, L. E. Borges da Silva and G. Lambert-Torres, "Smart impedance: a new way to look at hybrid filters," *IEEE Trans. Smart Grid*, vol. 7, no. 2, pp. 837-846, March 2016.

[84] R. Inzunza and H. Akagi, "A 6.6-kV transformerless shunt hybrid active filter for installation on a power distribution system," *IEEE Trans. Power Electron.*, vol. 20, no. 4, pp. 893-900, July 2005.

[85] H. Fujita, T. Yamasaki and H. Akagi, "A hybrid active filter for damping of

harmonic resonance in industrial power systems," *IEEE Trans. Power Electron.*, vol. 15, no. 2, pp. 215-222, Mar 2000.

[86] S. Rahmani, A. Hamadi, N. Mendalek and K. Al-Haddad, "A new control technique for three-phase shunt hybrid power filter," *IEEE Trans. Ind. Electron.*, vol. 56, no. 8, pp. 2904-2915, Aug. 2009.

[87] L. Herman, I. Papic and B. Blazic, "A proportional-resonant current controller for selective harmonic compensation in a hybrid active power filter," *IEEE Trans. Power Del.*, vol. 29, no. 5, pp. 2055-2065, Oct. 2014.

[88] L. Asiminoaei, W. Wiechowski, F. Blaabjerg, T. Krzeszowiak and B. Kedra, "A new control structure for hybrid power filter to reduce the inverter power rating," in *Proc. IEEE 32nd Ind. Electron. Soc. Annu. Conf., Paris, France*, Nov. 6–10, 2006, pp. 2712-2717.

[89] B. Kędra, "Reducing inverter power rating in active power filters using proposed hybrid power filter topology," in *Proc. 2015 IEEE EEEIC*, Rome, 2015, pp. 443-448.

[90] D. Jiang and F. Wang, "Variable switching frequency PWM for three-phase converter for loss and EMI improvement," in *Proc. IEEE APEC*, 2012, pp. 1576-1583.

[91] X. Mao, R. Ayyanar and H. K. Krishnamurthy, "Optimal variable switching frequency scheme for reducing switching loss in single-phase inverters based on time-domain ripple analysis," *IEEE Trans. Power Electron.*, vol. 24, no. 4, pp. 991-1001, April 2009.

[92] D. Jiang and F. Wang, "Variable switching frequency PWM for three-phase converters based on current ripple rrediction," *IEEE Trans. Power Electron.*, vol. 28, no. 11, pp. 4951-4961, Nov. 2013.

[93] J. Yin, S. Duan and B. Liu, "Stability analysis of grid-connected inverter with LCL filter adopting a digital single-loop controller with inherent damping characteristic," *IEEE Trans. Ind. Informat.*, vol. 9, no. 2, pp. 1104-1112, May 2013.

[94] J. He, Y. W. Li, D. Bosnjak and B. Harris, "Investigation and active damping of multiple resonances in a parallel-inverter-based microgrid," *IEEE Trans. Power Electron.*, vol. 28, no. 1, pp. 234-246, Jan. 2013.

[95] S. G. Parker, B. P. McGrath and D. G. Holmes, "Regions of active camping control for LCL filters," *IEEE Trans. Ind. Appl.*, vol. 50, no. 1, pp. 424-432, Jan.-Feb. 2014.

[96] E. Ebrahimzadeh, F. Blaabjerg, X. Wang and C. Leth Bak, "Efficient approach for harmonic resonance identification of large Wind Power Plants," in *Proc. IEEE PEDG*, 2016, pp. 1-7.

[97] Y. Wang, X. Wang, F. Blaabjerg and Z. Chen, "Harmonic instability assessment using state-space modeling and participation analysis in inverter-fed power systems," *IEEE Trans. Ind. Electron.*, vol. 64, no. 1, pp. 806-816, Jan. 2017.

[98] M. Lu, X. Wang, P. C. Loh and F. Blaabjerg, "Resonance interaction of multiparallel grid-connected inverters with LCL filter," *IEEE Trans. Power Electron.*, vol. 32, no. 2, pp. 894-899, Feb. 2017.

[99] S. Hiti, D. Boroyevich and C. Cuadros, "Small-signal modeling and control of three-phase PWM converters," in *Proc. Ind. Appl. Soc. Annu. Meeting*, Oct. 1994, vol. 2, pp. 1143–1150.

[100] Q. Ye, R. Mo, Y. Shi and H. Li, "A unified impedance-based stability criterion (UIBSC) for paralleled grid-tied inverters using global minor loop gain (GMLG)," in *Proc. IEEE ECCE*, 2015, pp. 5816-5821.

[101] C. Yoon, X. Wang, F. M. F. D. Silva, C. L. Bak and F. Blaabjerg, "Harmonic stability assessment for multi-paralleled, grid-connected inverters," in *Proc. IEEE APEC*, 2014, pp. 1098-1103.

[102] R. Peña-Alzola, M. Liserre, F. Blaabjerg, R. Sebastián, J. Dannehl and F. W. Fuchs, "Analysis of the passive damping losses in LCL-filter-based grid Converters," *IEEE Trans. Power Electron.*, vol. 28, no. 6, pp. 2642-2646, June 2013.

[103] J. Xu, S. Xie and T. Tang, "Active damping-based control for grid-connected LCL-filtered inverter with injected grid current feedback only," *IEEE Trans. Ind. Electron.*, vol. 61, no. 9, pp. 4746-4758, Sept. 2014.

[104] D. Pan, X. Ruan, C. Bao, W. Li and X. Wang, "Capacitor-current-feedback active damping with reduced computation delay for improving robustness of LCL-type grid-connected inverter," *IEEE Trans. Power Electron.*, vol. 29, no. 7, pp. 3414-3427, July 2014.

[105] X. Wang, F. Blaabjerg and P. C. Loh, "Virtual RC damping of LCL-filtered voltage source converters with extended selective harmonic compensation," *IEEE Trans. Power Electron.*, vol. 30, no. 9, pp. 4726-4737, Sept. 2015.

[106] W. L. Ming, Q. C. Zhong and X. Zhang, "A single-phase four-switch rectifier with significantly reduced capacitance," *IEEE Trans. Power Electron.*, vol. 31, no. 2, pp. 1618-1632, Feb. 2016.

[107] J. Dannehl, F. W. Fuchs, S. Hansen and P. B. Thogersen, "Investigation of active damping approaches for PI-based current control of grid-connected pulse width modulation converters with LCL filters," *IEEE Trans. Ind. Appl.*, vol. 46, no. 4, pp. 1509-1517, July-Aug. 2010.

[108] Z. Xin, P. C. Loh, X. Wang, F. Blaabjerg and Y. Tang, "Highly accurate derivatives for LCL-filtered grid converter with capacitor voltage active

damping," *IEEE Trans. Power Electron.*, vol. 31, no. 5, pp. 3612-3625, May 2016.

[109] X. Wu, X. Li, X. Yuan and Y. Geng, "Grid harmonics suppression scheme for LCL-type grid-connected inverters based on output admittance revision," *IEEE Trans. Sustain. Energy*, vol. 6, no. 2, pp. 411-421, April 2015.

[110] Z. Xin, X. Wang, P. C. Loh, F. Blaabjerg, "Grid-current feedback control for LCL-filtered grid converters with enhanced stability," *IEEE Trans. Power Electron.*, vol. 32, no. 4, pp. 3216-3228, April 2017.

[111] C. Chen, J. Xiong, Z. Wan, J. Lei and K. Zhang, "A time delay compensation method based on area equivalence for active damping of an LCL -type converter," *IEEE Trans. Power Electron.*, vol. 32, no. 1, pp. 762-772, Jan. 2017.

[112] X. Wang, Y. Pang, P. C. Loh and F. Blaabjerg, "A series-LC-filtered active damper with grid disturbance rejection for AC power-electronics-based power systems," *IEEE Trans. Power Electron.*, vol. 30, no. 8, pp. 4037-4041, Aug. 2015.

[113] X. Wang, F. Blaabjerg and M. Liserre, "An active damper to suppress multiple resonances with unknown frequencies," in *Proc. IEEE APEC*, 2014, pp. 2184-2191.

[114] D. Lu, X. Wang, H. Bai, and F. Blaabjerg, “A Sseries active damper with closed-loop control for sabilizing single-phase power-eectronics–based power system.”, In *Proc. IEEE ECCE*, 2016, pp. 1-7.

[115] N. Vazquez, D. Rico, C. Hernandez, R. Orosco and J. Arau, "Line current stabilizer based on a current active power filter," in *Proc. IEEE ISIE*, 2008, pp. 420-424.

[116] H. Fujita, T. Yamasaki and H. Akagi, "A hybrid active filter for damping of harmonic resonance in industrial power systems," *IEEE Trans. Power Electron.*, vol. 15, no. 2, pp. 215-222, Mar 2000.

[117] H. Liu, Y. Xing and H. Hu, "Enhanced frequency-locked loop with a comb filter under adverse grid conditions," *IEEE Trans. Power Electron.*, vol. 31, no. 12, pp. 8046-8051, Dec. 2016.

[118] H. Bai, X. Wang and F. Blaabjerg, "Passivity enhancement in renewable energy source based power plant with paralleled grid-connected VSIs," *IEEE Trans. Ind. Appl*, vol. 53, no. 4, pp. 3793-3802, July-Aug. 2017.

[119] H. Bai, X. Wang, P. C. Loh and F. Blaabjerg, "Passivity enhancement of grid-tied converters by series LC-filtered active damper," *IEEE Trans. Ind. Electron.*, vol. 64, no. 1, pp. 369-379, Jan. 2017.

[120] H. Bai, X. Wang, P. C. Loh and F. Blaabjerg, "An active trap filter for

switching harmonics attenuation of low-pulse-ratio inverters," *IEEE Trans. Power Electron.*, early access.

[121] H. Bai, X. Wang, P. C. Loh and F. Blaabjerg, "Harmonic analysis and mitigation of low-frequency switching voltage source inverter with series LC filtered VSI," *IEEE J. Emerg. Sel. Topics Power Electron.*, submitted.

[122] H. Bai, X. Wang, and F. Blaabjerg, "A grid-voltage-sensorless resistive active power filter with series LC-filter" *IEEE Trans. Power Electron.*, early access.

ISSN (online): 2446-1636
ISBN (online): 978-87-7112-987-8

AALBORG UNIVERSITY PRESS